

**Design of Passive Exotendon Spring Elements to Replace Muscle Torque
During Gait**

BY

BEATRICE MALIZIA
B.S., Politecnico di Milano, Milan, Italy, 2018

THESIS

Submitted as partial fulfillment of the requirements
for the degree of Master of Science in Bioengineering
in the Graduate College of the
University of Illinois at Chicago, 2021

Chicago, Illinois

Defense Committee:

James L. Patton, Chair and Advisor

Ming Wu, Bioengineering

Carlo Albino Frigo, Politecnico di Milano

ACKNOWLEDGMENTS

I would like to express my sincere gratitude to Dr. Jim Patton, for accepting to be my Advisor, for his continuous support and guidance and for giving me the opportunity to join his laboratory at the Shirley Ryan AbilityLab. His valuable advice allowed me to learn so much about the world of research and to achieve results beyond my expectations.

I would like to thank Professor Carlo Albino Frigo as well, for his insightful comments, precious contribution and encouragement. A special thanks also to Partha Ryali, who worked with me at the Shirley Ryan AbilityLab and really helped me during my research work.

Thanks to all the friends who have been close to me in this American adventure, you have made me feel close to home even when being so far.

Thanks to my Viminale family, many years have passed since when we were all together, but you will always be in my heart.

Thanks to my parents, who have always helped me and supported every decision I made, who taught me how to face life, who taught me what real love is, who always believe in me.

Thank you to my Grandpa, who have loved me and respected me from the very beginning.

BM

CONTRIBUTION OF AUTHORS

Chapter 1 is a literature review that places my Thesis question in the context of the larger field and highlights the significance of my research question. Chapter 2 presents the fundamentals behind my research and the main idea that started the work, had by my Advisor, Dr. James Patton. I generated Figures 1, 2, 3, 4. Chapters 3, 4, 5, 6, 7 represents a published manuscript [Malizia, B., Ryali, P., and Patton, J. L.: *Passive Exotendon Spring Elements can replace Muscle Torque during Gait. In 2020 8th IEEE RAS/EMBS International Conference for Biomedical Robotics and Biomechatronics (BioRob), pages 773-778, 2020.*] for which I was the primary author and major driver of the research. Partha Ryali assisted me in the initial development of the optimization algorithm shown in Chapter 4. My research Advisor, Dr. James Patton contributed to the writing of the manuscript and oversaw the development of the research. Chapter 7 also contains a series of my own unpublished experiments directed at answering the question of whether it is possible to use diagonal tension elements to reproduce any desired torque profile. I anticipate that this line of research will be continued in the laboratory after I leave and that this work will ultimately be published as part of a coauthored manuscript.

TABLE OF CONTENTS

<u>CHAPTER</u>		<u>PAGE</u>
1	INTRODUCTION	1
1.1	Gait Assistance and Rehabilitation	1
1.2	Robotic Exoskeletons	2
1.3	Using Springs to Assist Walking: Spring-Exoskeletons	2
1.4	Motivation	3
2	BACKGROUND: FROM THE MARIONET TO THE EXONET	5
2.1	The MARIONET	5
2.1.1	Two-joint MARIONET	7
2.2	The ExoNET	8
3	MUSCULAR TORQUE DEMAND FOR THE WALKING CYCLE	11
3.1	Data provided by David Winter, 2009	12
3.2	Data provided by Bovi et al., 2011	15
4	OPTIMIZATION ALGORITHM	19
4.1	Simulation Model	19
4.2	Set Up of the Algorithm	23
4.3	'Cost' function and Minimization Problem	24
4.4	ExoNET Simulated Torque Field	25
4.5	Simulated Annealing	26
4.6	Steps of the Optimization Algorithm	28
5	RESULTS OF THE OPTIMIZATION	30
5.1	Optimization Results for David Winter's data	30
5.1.1	One-element ExoNET System	31
5.1.2	Two-element ExoNET System	33
5.1.3	Three-element ExoNET System	35
5.1.4	Error Distribution	37
5.2	Optimization Results for Bovi et al.'s data	38
5.2.1	One-element ExoNET System	39
5.2.2	Two-element ExoNET System	41
5.2.3	Three-element ExoNET System	43
5.2.4	Error Distribution	45
5.3	Sensitivity Analysis	46
6	DISCUSSION	49

TABLE OF CONTENTS (continued)

<u>CHAPTER</u>		<u>PAGE</u>
	6.1 Optimization Results	49
	6.2 Error Distribution	49
	6.3 Sensitivity Analysis	50
	6.4 Conclusion	50
7	FUTURE WORK	52
	7.1 Dynamic Simulation	52
	7.2 Preliminary Prototype of the ExoNET	53
	APPENDIX	58
	CITED LITERATURE	59
	VITA	62

LIST OF FIGURES

<u>FIGURE</u>	<u>PAGE</u>
1 Basic concept of the MARIONET: by changing the moment arm, namely the distance between the Center of Rotation (CoR) and the point where the diagonal tension element is attached, one can control the generated torque.	6
2 MARIONET applied to the leg. R is the distance between the joint's CoR and the point where the diagonal tension element is attached, θ is the angle between R and the vertical, L is the length of the leg and Φ is the angle between the leg and the vertical.	7
3 Basic concept of the ExoNET: by stacking several MARIONETs in parallel, one can approximate torque profiles more complex than a sinusoid.	9
4 ExoNET applied to the leg. R is the distance between the joint's CoR and the point where the diagonal tension element is attached, θ is the angle between R and the vertical, L is the length of the leg and Φ is the angle between the leg and the vertical.	10
5 Torque field produced by the muscles of the right leg of a healthy person during walking at each combination of hip and knee angles. The horizontal component of the red arrows is the hip moment of force and the vertical component is the knee moment of force. Hip and knee angles are referred to the vertical line. The points of TOR (Toe Off Right) and of HCR (Heel Contact Right) with the associated swing and stance phases are highlighted. Data provided by David Winter, 2009.	13
6 Torque field produced by the right leg of a healthy person during walking with respect to the percentage of gait cycle. Hip Flexion and Knee Extension are positive. The points of TOR (Toe Off Right) and of HCR (Heel Contact Right) are highlighted. Data provided by David Winter, 2009.	14
7 Average torque field produced by the muscles of the leg of 20 adult healthy subjects, aged between 22 and 72, during natural speed gait, at each combination of hip and knee angles. The horizontal component of the red arrows is the hip moment of force and the vertical component is the knee moment of force. Hip and knee angles are referred to the vertical line. The swing and stance phases are highlighted. Data provided by Bovi et al., 2011.	16
8 Average torque field produced by the muscles of the leg of 20 adult healthy subjects, aged between 22 and 72, during natural speed gait, with respect to the percentage of gait cycle. Hip Flexion and Knee Extension are positive. Data provided by Bovi et al., 2011.	17
9 Comparison between David Winter's dataset and Bovi's dataset. . .	18

LIST OF FIGURES (continued)

<u>FIGURE</u>		<u>PAGE</u>
10	Schematic model of the elastic elements (in blue, green and orange) composing the ExoNET for a right leg. Each elastic element exerts a pulling tension T on the respective joint. $L1$ is the distance between the hip and the knee, $L2$ is the distance between the knee and the ankle, $\Phi1$ is the angle between $L1$ and the vertical, $\Phi2$ is the angle between $L1$ and $L2$, R is the distance between the Center of Rotation (CoR) and the point of attachment of the elastic element, θ is the angle between R and the vertical. ©2020 IEEE.	21
11	Sign convention adopted for the joint torques. Flexor moments about the hip joint and extensor moments about the knee joint are positive moments of force. ©2020 IEEE.	22
12	Flowchart of the optimization algorithm. The three inputs (red ovals) to the algorithm were: the number N of stacked MARIONETs, the set of initial parameters (R , θ , L_0) for each MARIONET, contained in a vector of length $N \cdot M$, being M the number of parameters for each element, and the desired torque field to approximate. The output (green shape) of the algorithm was the set of optimal parameters to approximate the desired torque field.	29
13	Arrangement of the one-element ExoNET system and associated torques generated by the device. To the left, a schematic of the body and the arrangement of the ExoNET, to the right, the torques created by the device (in blue) and the desired torques (in red). The joints (shoulder, hip, knee and ankle) are represented as black dots. Each MARIONET is represented as a line of a different color (blue, green and orange). . .	31
14	Torque field produced by the right leg of a healthy person during walking (in red) and simulated torque field generated by the one-element ExoNET system (in blue) with respect to the percentage of gait cycle. The points of TOR (Toe Off Right) and of HCR (Heel Contact Right) are highlighted.	32
15	Arrangement of the two-element ExoNET system and associated torques generated by the device. To the left, a schematic of the body and the arrangement of the ExoNET, to the right, the torques created by the device (in blue) and the desired torques (in red). The joints (shoulder, hip, knee and ankle) are represented as black dots. Each MARIONET is represented as a line of a different color (blue, green and orange). . .	33
16	Torque field produced by the right leg of a healthy person during walking (in red) and simulated torque field generated by the two-element ExoNET system (in blue) with respect to the percentage of gait cycle. The points of TOR (Toe Off Right) and of HCR (Heel Contact Right) are highlighted.	34

LIST OF FIGURES (continued)

<u>FIGURE</u>		<u>PAGE</u>
17	Arrangement of the three-element ExoNET system and associated torques generated by the device. To the left, a schematic of the body and the arrangement of the ExoNET, to the right, the torques created by the device (in blue) and the desired torques (in red). The joints (shoulder, hip, knee and ankle) are represented as black dots. Each MARIONET is represented as a line of a different color (blue, green and orange).	35
18	Torque field produced by the right leg of a healthy person during walking (in red) and simulated torque field generated by the three-element ExoNET system (in blue) with respect to the percentage of gait cycle. The points of TOR (Toe Off Right) and of HCR (Heel Contact Right) are highlighted.	36
19	Knee torque error (difference between the knee desired torques and the knee actual torques) versus hip torque error (difference between the hip desired torques and the hip actual torques) for the different configurations of the ExoNET system. Each point represents an instant of the gait cycle.	37
20	Arrangement of the one-element ExoNET system and associated torques generated by the device. To the left, a schematic of the body and the arrangement of the ExoNET, to the right, the torques created by the device (in blue) and the desired torques (in red). The joints (shoulder, hip, knee and ankle) are represented as black dots. Each MARIONET is represented as a line of a different color (blue, green and orange). . .	39
21	Torque field produced by the right leg of a healthy person during walking (in red) and simulated torque field generated by the one-element ExoNET system (in blue) with respect to the percentage of gait cycle. The points of TOR (Toe Off Right) and of HCR (Heel Contact Right) are highlighted.	40
22	Arrangement of the two-element ExoNET system and associated torques generated by the device. To the left, a schematic of the body and the arrangement of the ExoNET, to the right, the torques created by the device (in blue) and the desired torques (in red). The joints (shoulder, hip, knee and ankle) are represented as black dots. Each MARIONET is represented as a line of a different color (blue, green and orange). . .	41
23	Torque field produced by the right leg of a healthy person during walking (in red) and simulated torque field generated by the two-element ExoNET system (in blue) with respect to the percentage of gait cycle. The points of TOR (Toe Off Right) and of HCR (Heel Contact Right) are highlighted.	42

LIST OF FIGURES (continued)

<u>FIGURE</u>		<u>PAGE</u>
24	Arrangement of the three-element ExoNET system and associated torques generated by the device. To the left, a schematic of the body and the arrangement of the ExoNET, to the right, the torques created by the device (in blue) and the desired torques (in red). The joints (shoulder, hip, knee and ankle) are represented as black dots. Each MARIONET is represented as a line of a different color (blue, green and orange).	43
25	Torque field produced by the right leg of a healthy person during walking (in red) and simulated torque field generated by the three-element ExoNET system (in blue) with respect to the percentage of gait cycle. The points of TOR (Toe Off Right) and of HCR (Heel Contact Right) are highlighted.	44
26	Knee torque error (difference between the knee desired torques and the knee actual torques) versus hip torque error (difference between the hip desired torques and the hip actual torques) for the different configurations of the ExoNET system. Each point represents an instant of the gait cycle.	45
27	Average magnitude of the error, namely the difference between the desired torques and the actual torques, across all the perturbation combinations. The non-distorted configuration (5) is highlighted in red. . .	47
28	Arrangement of the two-element ExoNET system for different combinations of perturbation on the desired torque field.	48
29	Physical non-functional prototype of the ExoNET made by one elastic element per joint. The parameters that can be adjusted on the ExoNET are indicated in red. ©2020 IEEE.	54
30	Physical non-functional prototype of the ExoNET made by two elastic elements per joint.	55

LIST OF ABBREVIATIONS

ADLs	Activities of Daily Living
CoR	Center of Rotation
CT	Conventional Training
ExoNET	Exoskeletal Network for Elastic Torque
MARIONET	Moment Arm Adjustment for Remote Induction of Net Effective Torque
QOL	Quality of Life
RAGT	Robot-Assisted Gait Training
SA	Simulated Annealing
SKG	Stiff-Knee Gait

SUMMARY

”Nowadays, wearable exoskeletons are widely used as assistive tools during gait rehabilitation, implementing strategies such as gravity compensation and metabolic cost reduction, however, these devices often require the use of motors and controllers. This research is driven by the need for a simple, inexpensive and customizable device, a passive exotendon able to provide a desired torque profile to multiple joints. A simulation model study was implemented to see whether it is possible to use diagonal tension elements, which act mathematically as basis functions, to reproduce the torque field generated by a healthy person during walking. This would allow to create a wearable exotendon system made of passive elastic elements able to deliver this torque field to the lower extremity of the patient during gait rehabilitation. The results presented in this work show that it is indeed possible to create a passive torque field from elastic elements that approximates the muscular torque demand for the walking cycle. This represents a starting point for the design of a passive exotendon capable of providing assistive torques to patients with motor deficits, thus reducing the metabolic cost of walking.” [1]

©2020 IEEE

CHAPTER 1

INTRODUCTION

1.1 Gait Assistance and Rehabilitation

Impairments in lower limb motor function often leads to a significant decrease in the Quality of Life (QOL) [2] and they can have various causes, such as stroke and spinal cord injury. In this context, gait assistance and rehabilitation are key steps for patients survived a stroke or an injury who are experiencing neuromuscular dysfunction leading to a decrease in mobility, giving them the possibility to recover, at least partially, the ability to perform Activities of Daily Living (ADLs), thus improving their Quality of Life.

Nowadays, wearable exoskeletons are widely used in clinical settings as assistive tools for improving walking ability during assistance and rehabilitation, allowing patients with motor deficits to sustain repetitive and intense gait training and to regain mobility. The performance of locomotor training, consisting of repetitions of task-oriented exercises through Robot-Assisted Gait Training (RAGT) in combination with Conventional Training (CT), has been shown to improve the positive effect on the ambulation abilities of the patient [3]. Whole body motion support mobile suits have been developed to help patients recover physiologic gait while minimizing the risk of falling [4]. Many other devices have been designed to make gait easier, implementing strategies such as gravity compensation and metabolic cost reduction. Here, it's recognized that, although these devices can be active (requiring motors, sensors, computers and

power) they can also be passive: rather than using external sources to inject energy and reduce patient work, passive devices may be able to intelligently recycle energy.

1.2 Robotic Exoskeletons

Some devices for gait rehabilitation come in the form of wearable robotic exoskeletons, such as the Lokomat by Hocoma [5], an adjustable exoskeleton for robot-assisted gait therapy, intended to overcome the limitations of manual treadmill training. Other examples are the Ekso Bionics' exoskeleton, able to let paraplegic patients walk [6], and the ReWalk, that supplies powered hip and knee motion to allow patients with spinal cord injury to move [7]. However, all these robotic devices have the characteristic of being intimidating, bulky, complex and expensive. They require the use of motors, controllers, sensors and may not be used by therapists because of the extra time they would need to learn how to use them, set them up and deal with any arising problems.

1.3 Using Springs to Assist Walking: Spring-Exoskeletons

An alternative solution consists in fully-passive wearable devices made of springs, that can be adjusted to the geometry of the leg. Springs allow to make gait easier, for example, it has been shown by Simpson's group that the use of an Exotendon made of springs connecting the legs improves human running economy, reducing the energy required for running by about 6%, by applying assistive forces to the swinging legs [8]. One assistive strategy for gait, implemented by these spring-exoskeletons, is gravity compensation, which aims at reducing the

weight applied to the leg joints during motion, and is provided by systems as the one presented by Agrawal’s group [9]. They developed a spring-exoskeleton able to unload the leg joints from gravity, decreasing the engagement of the muscles by 25% and increasing the range of motion at the hip and knee joints. Another target of such systems is metabolic cost reduction, by making spring mechanisms that store and return energy during the gait cycle. Prominent examples are an unpowered clutch-spring system, developed by Collins’ group, that has been shown to reduce the oxygen consumption during healthy gait by about 7% [10], and a passive exosuit to support balance control, developed by Barazesh’s group, able to reduce the metabolic cost of walking by 4% [11]. Another example is a device capable of assisting knee flexion torque before swing, developed by Patton’s group [12].

1.4 Motivation

Therapists are usually given short amounts of time to perform rehabilitation sessions with the patient. For this reason, they tend to prefer the use of rehabilitative and assistive technology that is quick to assemble, easy to use and easy to learn, so that they don’t have to dedicate an excessive amount of time to assemble the equipment. In this perspective, this study aims at developing a passive wearable device that does not require motors, controllers, sensors, or power, and therefore has the potential to be simple, inexpensive, adjustable, and easy to put on and take off. This wearable exotendon would be capable of delivering a desired torque profile to the joints of a patient by using a network of diagonal tension elements, such as springs. These

assistive torques are meant to help reduce the motor deficits of the patient by decreasing the engagement of muscles.

The idea of using springs to assist the movement of the legs takes inspiration from nature itself: in both animals and humans, we can find examples of spring-like tissues that are believed to assist leg swing and to save energy by offloading the muscles that swing the legs [8]. A study on the operating of the musculoskeletal spring system at different speeds in animals pointed out that the stiffness of the leg spring was nearly independent of speed in certain animals, since they bounce off the ground faster at higher speeds [13]. Thomas McMahon pointed out the spring-like properties of muscles in running, stating that potential energy is stored and reused in the form of elastic energy during the running cycle [14]. A pioneering idea of designing stiffness for walking and running comes from a study on experimental platforms with adjustable stiffness, tuned to minimize energy loss during impact and to see how leg stiffness and metabolic cost are impacted by changes in substrate stiffness [15]. With these premises, this study focuses on how simple springs can improve human walking economy.

CHAPTER 2

BACKGROUND: FROM THE MARIONET TO THE EXONET

Parts of this chapter were previously published as Malizia, B., Ryali, P., and Patton, J. L.: Passive Exotendon Spring Elements can replace Muscle Torque during Gait. In 2020 8th IEEE RAS/EMBS International Conference for Biomedical Robotics and Biomechatronics (BioRob), pages 773-778, 2020.

2.1 The MARIONET

This research is driven by the need for a simple, inexpensive and customizable device, able to provide a desired torque profile to multiple joints [1]. A first realization of this idea was the Moment Arm Adjustment for Remote Induction of Net Effective Torque (MARIONET), a device developed by Patton’s group based on the change of moment arm to control the generated torque [16], as shown in Figure 1. Basically, by moving the point of attachment of the elastic element at different positions with respect to the joint’s center of rotation, different torque profiles can be generated. The MARIONET overcomes the need for motors and controllers and for a rigid skeleton, using the very anatomy of the human body as a rigid link. This is a diagonal tension element that generates a sinusoidal torque profile, and so it acts mathematically as a basis function. By stacking more MARIONETs in parallel, it’s possible to approximate complex torque fields, and not only sinusoidal ones. In particular, this study wanted to use this network

of diagonal tension elements to reproduce the torque field generated by a healthy person during walking.

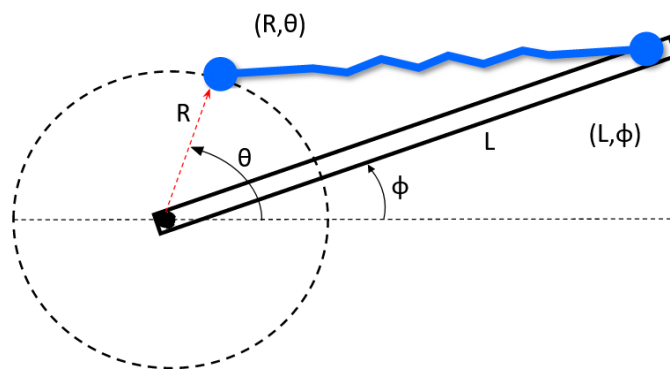


Figure 1: Basic concept of the MARIONET: by changing the moment arm, namely the distance between the CoR and the point where the diagonal tension element is attached, one can control the generated torque.

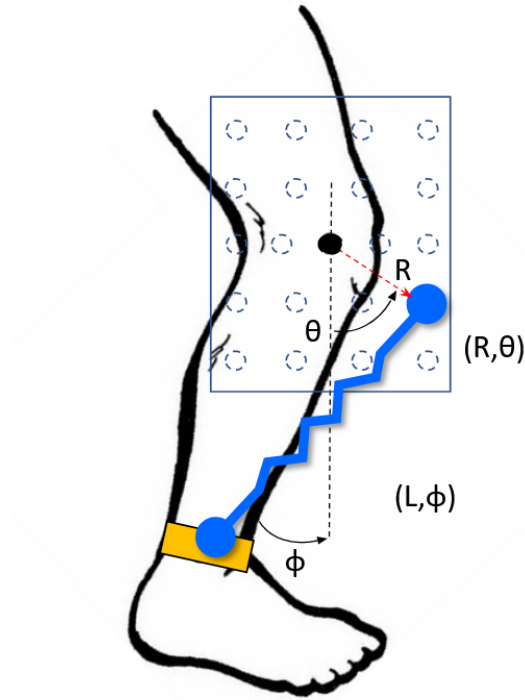


Figure 2: MARIONET applied to the leg. R is the distance between the joint's CoR and the point where the diagonal tension element is attached, θ is the angle between R and the vertical, L is the length of the leg and Φ is the angle between the leg and the vertical.

2.1.1 Two-joint MARIONET

Another version of the MARIONET can be created by linking directly the hip to the ankle through an elastic element, therefore obtaining a two-joint MARIONET. The idea comes from the structure of two-joint muscles, which can produce moments about two joints. The use of two-joint MARIONETs, in combination with one-joint MARIONETs, in a multi-link model,

could bring improvements to the final device. Indeed, it has been pointed out that bi-articular muscles play a unique role by distributing net joint moments and joint powers over the joints [17]. Moreover, it has been shown that, bi-articular muscles make movement coordination more efficient [18].

2.2 The ExoNET

In the present work, a device called Exoskeletal Network for Elastic Torque (ExoNET) is presented, realized by stacking several MARIONETs together across multiple joints [1]. The result is a multidimensional spring system, able to approximate torque profiles more complex than a sinusoid, where the overall torque generated by the device is the linear sum of the torques generated by each element.

$$\text{ExoNET Torques} = \sum_{i=1}^N \tau_i \quad (2.1)$$

Where ExoNET Torques is a two-column matrix containing the simulated torques for the hip (first column) and for the knee (second column) at each hip and knee angle combination, and τ_i are the torques generated by each one of the N MARIONETs.

A first design of the device was intended for the upper extremity [19], however, it has the potential to be used for the actuation of several joints, so it could also be implemented for the lower extremity [1]. The movement of the leg creates in the space a position-dependent non-linear function, that is a position-dependent torque in each joint, and therefore a multi-dimensional torque. Springs, because of their nature, are position-dependent as well, so an optimization function could be used to position them in a way to obtain the torque desired.

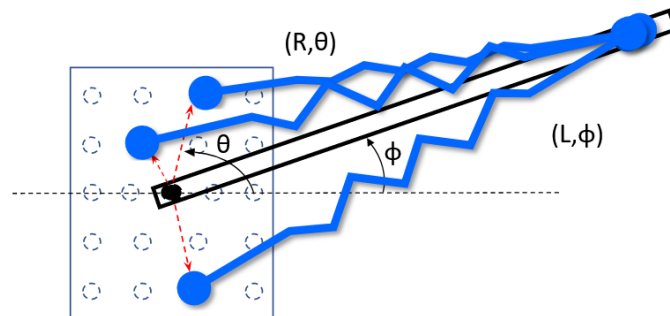


Figure 3: Basic concept of the ExoNET: by stacking several MARIONETs in parallel, one can approximate torque profiles more complex than a sinusoid.

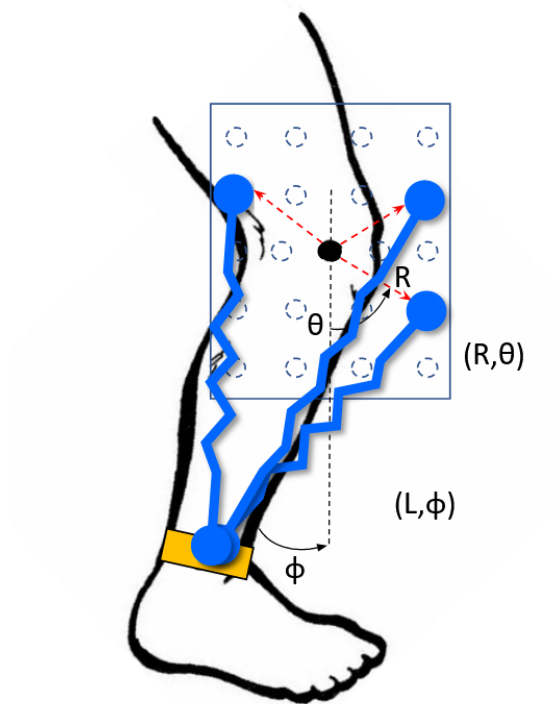


Figure 4: ExoNET applied to the leg. R is the distance between the joint's CoR and the point where the diagonal tension element is attached, θ is the angle between R and the vertical, L is the length of the leg and Φ is the angle between the leg and the vertical.

By stacking more MARIONETs in parallel, it's possible to approximate torque fields more complex than sinusoidal ones. In particular, this study wanted to use this network of diagonal tension elements to reproduce the torque field generated by a healthy person during walking.

CHAPTER 3

MUSCULAR TORQUE DEMAND FOR THE WALKING CYCLE

Parts of this chapter were previously published as Malizia, B., Ryali, P., and Patton, J. L.: Passive Exotendon Spring Elements can replace Muscle Torque during Gait. In 2020 8th IEEE RAS/EMBS International Conference for Biomedical Robotics and Biomechatronics (BioRob), pages 773-778, 2020.

This research aims at using a network of elastic elements, i.e. ideal springs, to approximate the muscular torque demand for the walking cycle [1]. For this purpose, data on the biomechanics of human movement were taken from the literature, in particular from David Winter’s book “Biomechanics and Motor Control of Human Movement” [20] and from Bovi et al.’s paper on the gait analysis for healthy young and adult subjects [21].

The physical quantities considered in this study were:

- Hip angles, in degrees.
- Knee angles, in degrees.
- Hip moments of force, in Newton-meters.
- Knee moments of force, in Newton-meters.

All these quantities were referred to healthy subjects during natural speed gait.

3.1 Data provided by David Winter, 2009

In Figure 5, the moments of force exerted by the muscles on the hip joint and on the knee joint, taken from David Winter's book [20], are shown in the plane formed by each combination of hip and knee angles during the gait cycle.

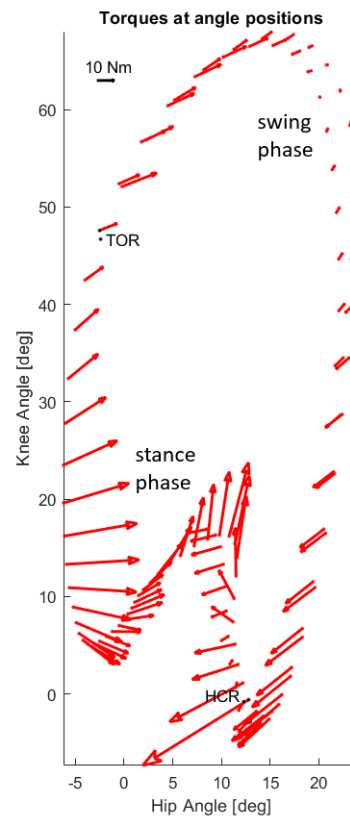


Figure 5: Torque field produced by the muscles of the right leg of a healthy person during walking at each combination of hip and knee angles. The horizontal component of the red arrows is the hip moment of force and the vertical component is the knee moment of force. Hip and knee angles are referred to the vertical line. The points of TOR (Toe Off Right) and of HCR (Heel Contact Right) with the associated swing and stance phases are highlighted. Data provided by David Winter, 2009.

In Figure 6, the same moments of force exerted by the hip muscles and by the knee muscles are represented with respect to the percentage of the gait cycle.

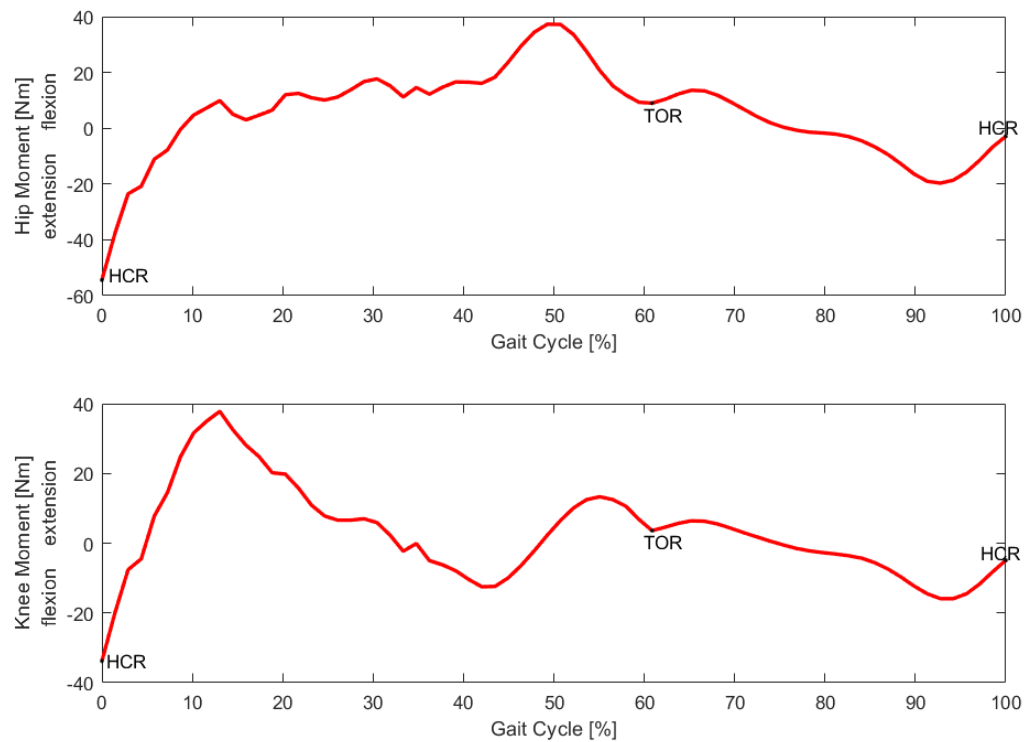


Figure 6: Torque field produced by the right leg of a healthy person during walking with respect to the percentage of gait cycle. Hip Flexion and Knee Extension are positive. The points of TOR (Toe Off Right) and of HCR (Heel Contact Right) are highlighted. Data provided by David Winter, 2009.

It can be seen that the torques needed during the stance phase are higher with respect to the torques required during the swing phase. This research aimed at trying to replicate such torques with the ExoNET device.

3.2 Data provided by Bovi et al., 2011

In Figure 7, the moments of force exerted by the muscles on the hip joint and on the knee joint, taken from Bovi's paper [21], are shown in the plane formed by each combination of hip and knee angles during the gait cycle.

In Figure 8, the same moments of force exerted by the hip muscles and by the knee muscles are represented with respect to the percentage of the gait cycle.

In Figure 9, the torque dataset provided by David Winter [20] and the torque dataset provided by Bovi et al. [21] are compared.

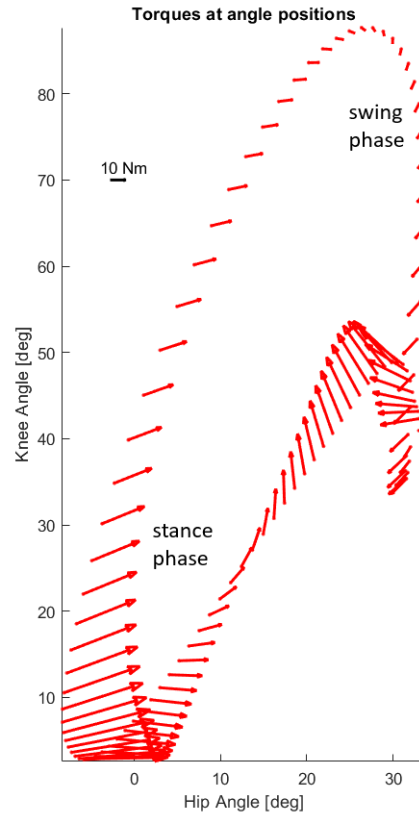


Figure 7: Average torque field produced by the muscles of the leg of 20 adult healthy subjects, aged between 22 and 72, during natural speed gait, at each combination of hip and knee angles. The horizontal component of the red arrows is the hip moment of force and the vertical component is the knee moment of force. Hip and knee angles are referred to the vertical line. The swing and stance phases are highlighted. Data provided by Bovi et al., 2011.

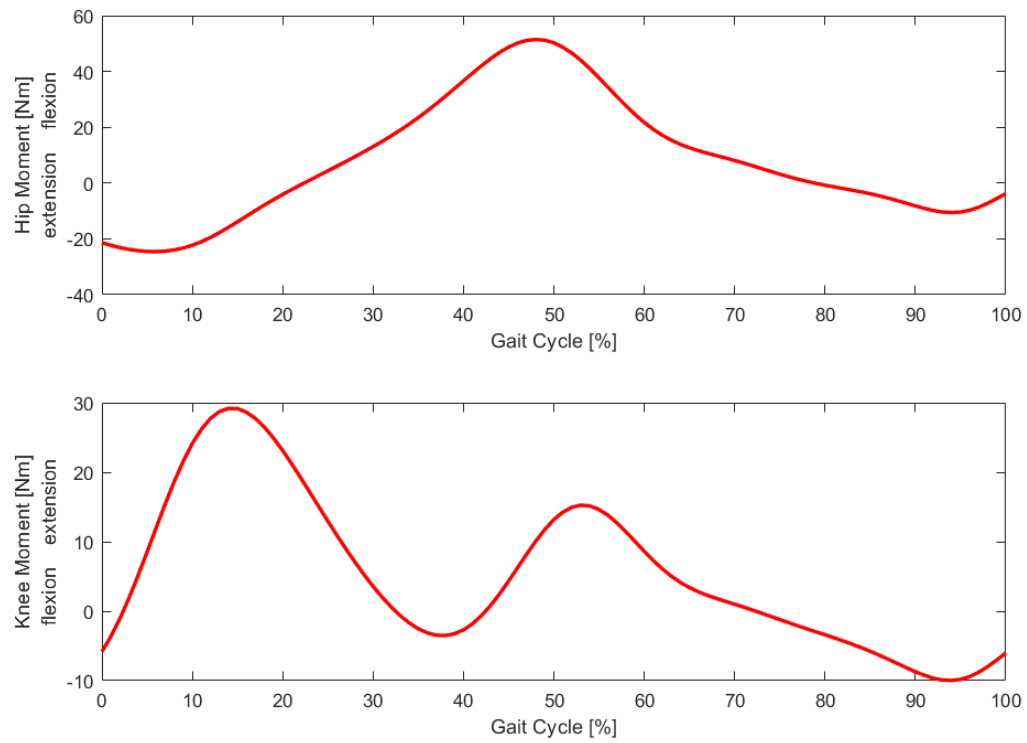


Figure 8: Average torque field produced by the muscles of the leg of 20 adult healthy subjects, aged between 22 and 72, during natural speed gait, with respect to the percentage of gait cycle. Hip Flexion and Knee Extension are positive. Data provided by Bovi et al., 2011.

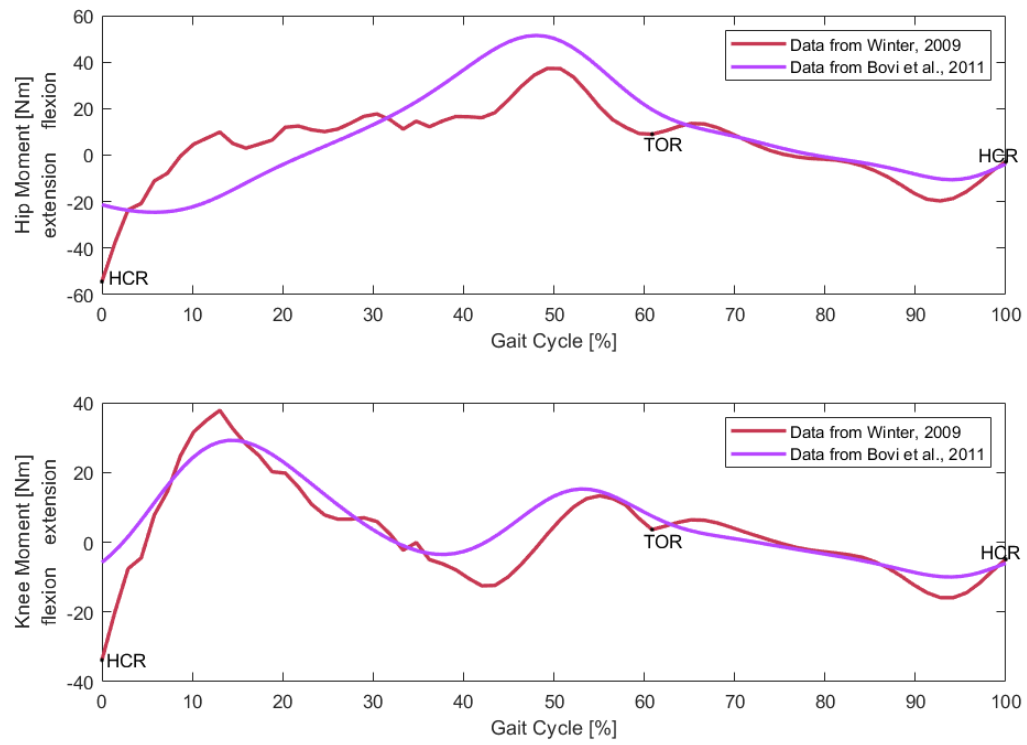


Figure 9: Comparison between David Winter's dataset and Bovi's dataset.

CHAPTER 4

OPTIMIZATION ALGORITHM

Parts of this chapter were previously published as Malizia, B., Ryali, P., and Patton, J. L.: Passive Exotendon Spring Elements can replace Muscle Torque during Gait. In 2020 8th IEEE RAS/EMBS International Conference for Biomedical Robotics and Biomechatronics (BioRob), pages 773-778, 2020.

This work shows that the use of optimization algorithms can contribute to selecting the best arrangement of a network made of diagonal tension elements to approximate the torques exerted by the muscles during walking [1]. Such network is called ExoNET and is made by stacking several MARIONETs in parallel, elastic elements based on the change of moment arm to control the generated torque. By stacking more elastic elements in parallel, we are creating a multidimensional spring system able to approximate any desired torque profile. This algorithm is based on the minimization of a defined 'cost' function, which will be explained more fully later, by using a derivative-free method combined with the perturbation algorithm of Simulated Annealing.

4.1 Simulation Model

This work presents the simulation model of a wearable, completely passive device made of elastic elements, i.e. ideal springs, which can deliver the muscular torque demand for the walking cycle to the joints of a patient during natural speed gait. A schematic model of the

ExoNET system is shown in Figure 10. This device is articulated around three joints, hip, knee and ankle, and is made by:

- One-joint elastic elements, connecting the hip to the knee (in blue) and connecting the knee to the ankle (in green).
- Two-joint elastic elements, connecting the hip to the ankle (in orange).

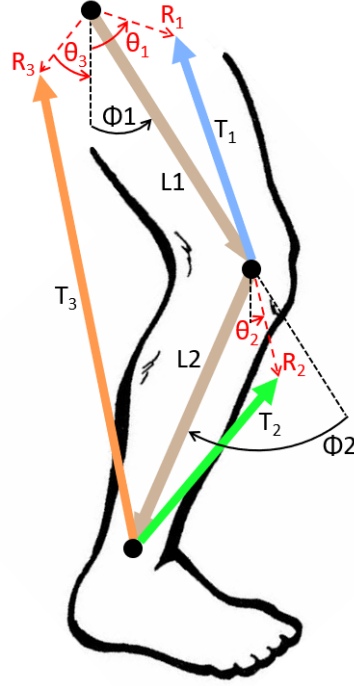


Figure 10: Schematic model of the elastic elements (in blue, green and orange) composing the ExoNET for a right leg. Each elastic element exerts a pulling tension T on the respective joint. $L1$ is the distance between the hip and the knee, $L2$ is the distance between the knee and the ankle, $\Phi1$ is the angle between $L1$ and the vertical, $\Phi2$ is the angle between $L1$ and $L2$, R is the distance between the Center of Rotation (CoR) and the point of attachment of the elastic element, θ is the angle between R and the vertical. ©2020 IEEE.

Each MARIONET is identified by three parameters:

- R is the distance between the joint's CoR and the point of attachment of the spring.

- θ is the angle between R and the vertical line.
- L_0 is the resting length of the spring.

Each elastic element is exerting a pulling tension T on the respective joint, whose magnitude is equal to the product of the spring stiffness and the displacement of the spring.

The sign convention adopted for the joint torques considered hip joint flexor moments and knee joint extensor moments as positive moments of force, as shown in Figure 11.

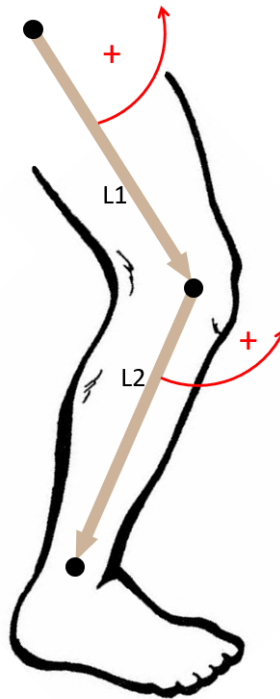


Figure 11: Sign convention adopted for the joint torques. Flexor moments about the hip joint and extensor moments about the knee joint are positive moments of force. ©2020 IEEE.

4.2 Set Up of the Algorithm

The MATLAB software was used to create a simulation model of the ExoNET and to implement an optimization algorithm able to find a set of optimal parameters (\mathbf{R} , θ , L_0) for each MARIONET, modeled as ideal springs. These sets of parameters describe how to arrange the elastic elements of the ExoNET to make it approximate the desired torque field [1].

In the first step, the anatomical parameters for the body were set. The lengths of the body segments, taken from anthropometric tables listed in David Winter's book [20], were referred to an average height of 1.70 m. While the spring stiffness for all the elastic elements was set to a value of 10,000 N/m, the number of stacked MARIONETs could be chosen by means of an input window after the start of the optimization. The higher the number of stacked elastic elements chosen, the higher the computational cost and the time needed to find the solution.

As already said, the output of the optimization algorithm was a set of parameters (\mathbf{R} , θ , L_0) for each MARIONET. Since this computational model was a simulation for a wearable device, there was the need to set some restrictions on the values that could be assumed by the parameters of the passive elastic elements forming the ExoNET. These restrictions were written as regularization terms, or soft constraints, by setting the minimum and maximum value that each parameter could assume. The parameter \mathbf{R} could not assume values higher than about 20 cm, otherwise the device would become too bulky and the comfort of the patient while wearing it would decrease, however, it was allowed to assume values around zero, this way it could be seen which elastic elements were to have a null moment arm and so wouldn't be necessary to include in the device. Indeed, the contribution of an elastic element, applied very close to the joint's

CoR, to the total torque generated by the device can be considered negligible and thus this elastic element may be removed from the device itself, making it lighter and more comfortable. As regards L_0 , its value was constrained between 5 cm and 30 cm. On the other hand, the value of θ didn't need to be constrained, since the angle is a periodic function, and so it could assume any value. The outcome of the optimization algorithm was dependent on the initialization of the problem and on the value of the constraints chosen for R , θ and L_0 .

4.3 'Cost' function and Minimization Problem

The optimization algorithm was based on the minimization of a defined 'cost' function, whose value was dependent on how much the estimated parameters (R , θ , L_0) differed from their acceptable ranges. To start the optimization, the initial values of R , θ and L_0 were chosen as the minimum value of their respective ranges. During each optimization try, the minimization of the 'cost' function was performed by using the function 'fminsearch', contained on the MATLAB Optimization Toolbox, able to solve nonlinear problems using a derivative-free method, and used to find the set of parameters (R , θ , L_0) corresponding to minima of the 'cost' function [1]. The initial 'cost' was calculated as the sum of the squares of the residuals, and the residuals were computed as the differences between the desired torques and the simulated torques created by the ExoNET:

$$\text{cost}_0 = \sum_{i=1}^n (\text{Desired Torques}_i - \text{ExoNET Torques}_i)^2 \quad (4.1)$$

Where n was the length of the **Desired Torques** matrix, whose first column contained the hip desired torques and whose second column contained the knee desired torques at each hip and knee angle combination, and of the **ExoNET Torques** matrix, whose first column contained the hip simulated torques and whose second column contained the knee simulated torques at each hip and knee angle combination. For every parameter (R, θ, L_0) , the initial ‘cost’ was increased by a **penalty**, given by the product of a positive constant λ and the absolute difference between the value of the parameter p and the upper bound p_0 of its acceptable range (if the value of the parameter was higher than the maximum acceptable value) or the lower bound p_0 of its acceptable range (if the value of the parameter was lower than the minimum acceptable value):

$$\text{penalty} = \lambda |p - p_0| \quad (4.2)$$

Therefore, by summing Equation 4.1 and Equation 4.2, the total ‘cost’ in each optimization try was equal to:

$$\text{cost} = \text{cost}_0 + \lambda |p - p_0| \quad (4.3)$$

4.4 ExoNET Simulated Torque Field

By knowing that the torque vector $\vec{\tau}$ is given by the cross product between the position vector of the point of application of the force \vec{r} and the vector of the applied force \vec{F} :

$$\vec{\tau} = \vec{r} \times \vec{F} \quad (4.4)$$

The torques generated by the elastic elements could be computed, by using as \vec{r} the distance between the CoR and the point where the spring was inserted and as \vec{F} the tension exerted by the spring. Considering the MARIONETs as ideal springs, the magnitude of the force F generated by each MARIONET could be computed through the Hooke's law as the product of the spring stiffness k and the displacement of the spring $L-L_0$, where L_0 was the resting length of the spring:

$$F = -k (L - L_0) \quad (4.5)$$

Since the MARIONETs can be considered as basis functions, the total torque generated by the ExoNET was obtained by summing all the torques τ_i generated by each one of the N MARIONETs:

$$\text{ExoNET Torques} = \sum_{i=1}^N \tau_i \quad (4.6)$$

The result called ExoNET Torques was a two-column matrix containing the simulated torques for the hip (first column) and for the knee (second column) at each hip and knee angle combination.

4.5 Simulated Annealing

This optimization algorithm was combined with the perturbation algorithm of Simulated Annealing (SA), used in minimization problems. The SA technique was used to kick away the starting parameters of each optimization try from the optimal values found at the end of the previous try. This prevented the algorithm from getting stuck in local minima of the ‘cost’

function. SA is a derivative-free method for approximating the global minimum of a non-linear function, over a large search space [22], preventing being trapped in local minima by using a random search [23]. This algorithm takes inspiration from the physical phenomena happening during the heat treatment of annealing in metallurgy, the process of heating up a solid, such as a metal, to a high temperature, followed by slow cooling in steps [24]. SA is a stochastic search technique, statistically granted to find the global optimal solution [24]. One characteristic of this technique is that the selection of the initial control parameters strongly influences the solution. However, this algorithm is also easy to implement, it is able to find a global optimal even after finding a local minimum and it can provide satisfactory results with a relatively low number of iterations [23].

In this technique, the solution space is searched by perturbing the estimates of the parameters to optimize (R, θ, L_0) [25]. These perturbations depend on the range of the parameter constraints and on the current number of iterations, and their magnitude at any stage in the optimization process is given by:

$$\text{pert}(P) = \text{range} \cdot (\text{nTries}/\text{TRY}) \cdot \text{randn} \quad (4.7)$$

Where $\text{pert}(P)$ is the perturbation on the estimates of the parameters (R, θ, L_0) , range is the range of each parameter (R, θ, L_0) , nTries is the total number of optimization reruns, TRY is the current number of iterations and randn is a vector of normally distributed pseudorandom numbers. The $(\text{nTries}/\text{TRY})$ ratio becomes smaller with each step, thus reducing the magnitude of the parameters perturbation as conditions come close to the optimum. Each set of parameters, obtained from this process, is substituted into the equations of the model. Then,

the performance of the set of parameters is evaluated through simulation. This evaluation of the performance concerns the comparison of the desired and the actual torque field, and is quantified using the 'cost'. If the value of the 'cost' is lower than the previous best 'cost', the new set of parameters replaces the previous set [25].

4.6 Steps of the Optimization Algorithm

To sum up, the implemented optimization algorithm followed these steps:

- Start with a preset initial vector of parameters $(\mathbf{R}, \theta, L_0)$ and assign a high 'cost' to the corresponding torque function.
- Starting from the previous parameters, find a new vector of parameters $(\mathbf{R}, \theta, L_0)$ corresponding to a local minimum of the 'cost' function through the 'fminsearch' function.
- If the values of the new parameters are higher or lower than the preset parameter constraints, increase the respective 'cost' by a positive constant.
- Randomly generate a new vector of parameters $(\mathbf{R}, \theta, L_0)$ and find the difference in the generated torque function.
- Determine whether the new vector of parameters is better, namely has a lower 'cost', or worse, namely has a higher 'cost', than the current one.
- If the new vector of parameters is accepted, store it.

All these steps were repeated for a preset number of iterations.

Figure 12 shows the flowchart of the computational steps implemented to find the optimal parameters.

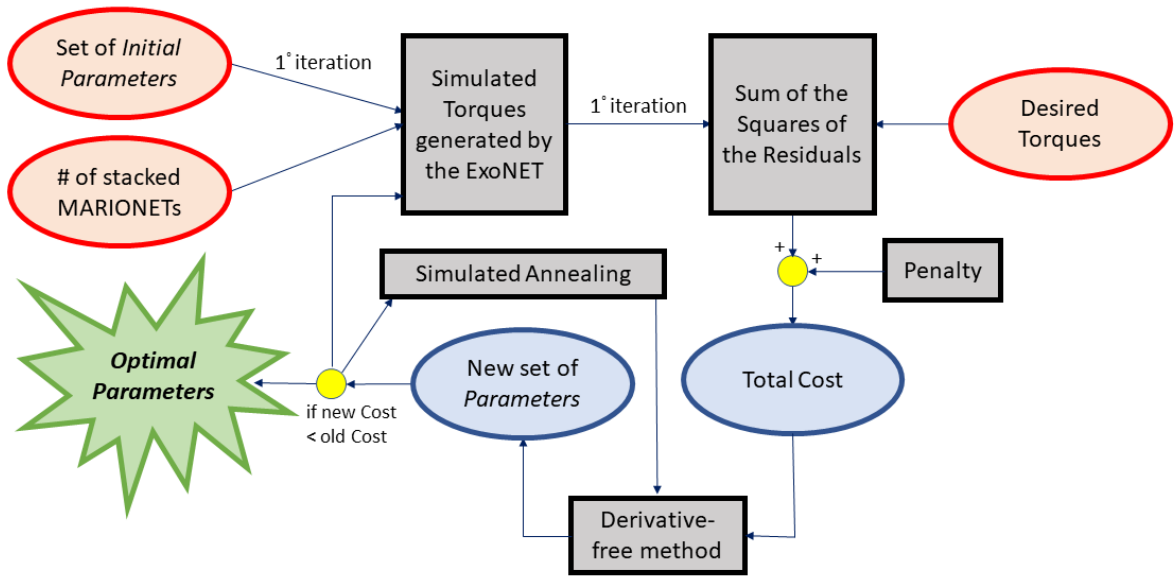


Figure 12: Flowchart of the optimization algorithm. The three inputs (red ovals) to the algorithm were: the number N of stacked MARIONETS, the set of initial parameters (R, θ, L_0) for each MARIONET, contained in a vector of length $N \cdot M$, being M the number of parameters for each element, and the desired torque field to approximate. The output (green shape) of the algorithm was the set of optimal parameters to approximate the desired torque field.

CHAPTER 5

RESULTS OF THE OPTIMIZATION

Parts of this chapter were previously published as Malizia, B., Ryali, P., and Patton, J. L.: Passive Exotendon Spring Elements can replace Muscle Torque during Gait. In 2020 8th IEEE RAS/EMBS International Conference for Biomedical Robotics and Biomechatronics (BioRob), pages 773-778, 2020.

In this chapter, the results obtained from the presented optimization algorithm are shown.

5.1 Optimization Results for David Winter's data

At first, the optimization algorithm was executed for an ExoNET system made of only one elastic element per joint, then the number of stacked MARIONETs was increased to two and three elastic elements per joint. A schematic of the human body is used to visualize how the elastic elements, in green, orange and blue, should be positioned on the lower extremity in order to provide the assistive torques to the joints. The torques created by such an arrangement of the device during the gait cycle are plotted in blue, while the desired torques are plotted in red. During the movement of the leg, the moment arm of the springs is rigid and remains in place, while the springs engage and disengage based on the joint's position.

5.1.1 One-element ExoNET System

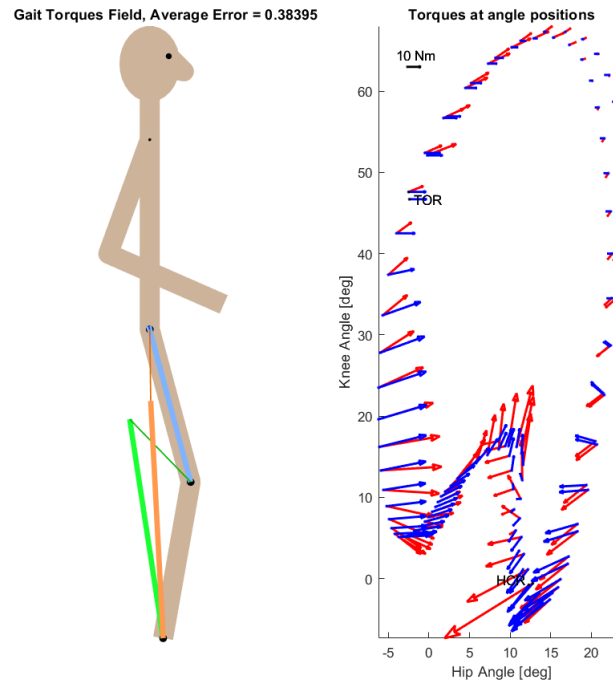


Figure 13: Arrangement of the one-element ExoNET system and associated torques generated by the device. To the left, a schematic of the body and the arrangement of the ExoNET, to the right, the torques created by the device (in blue) and the desired torques (in red). The joints (shoulder, hip, knee and ankle) are represented as black dots. Each MARIONET is represented as a line of a different color (blue, green and orange).

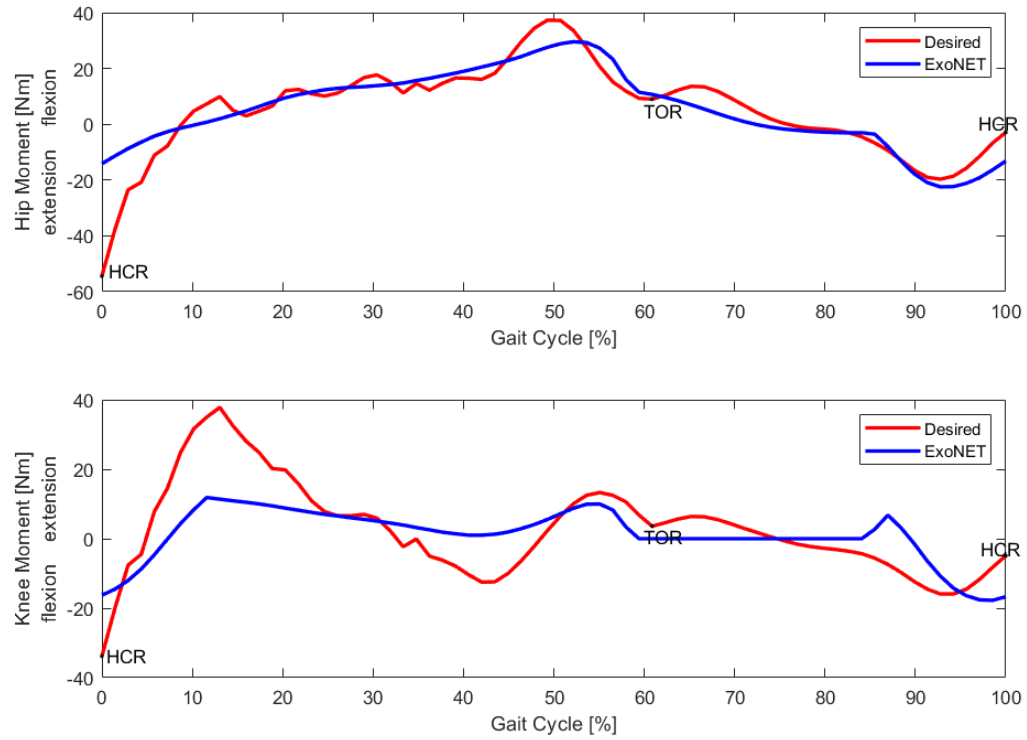


Figure 14: Torque field produced by the right leg of a healthy person during walking (in red) and simulated torque field generated by the one-element ExoNET system (in blue) with respect to the percentage of gait cycle. The points of TOR (Toe Off Right) and of HCR (Heel Contact Right) are highlighted.

5.1.2 Two-element ExoNET System

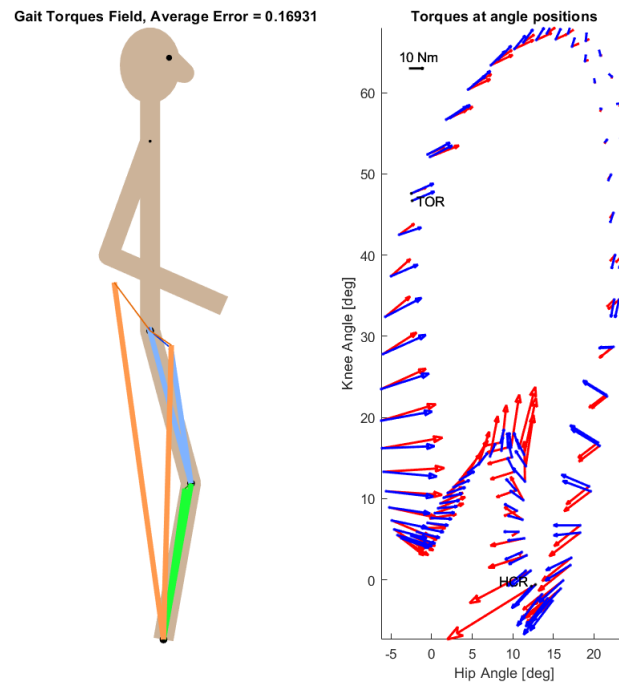


Figure 15: Arrangement of the two-element ExoNET system and associated torques generated by the device. To the left, a schematic of the body and the arrangement of the ExoNET, to the right, the torques created by the device (in blue) and the desired torques (in red). The joints (shoulder, hip, knee and ankle) are represented as black dots. Each MARIONET is represented as a line of a different color (blue, green and orange).

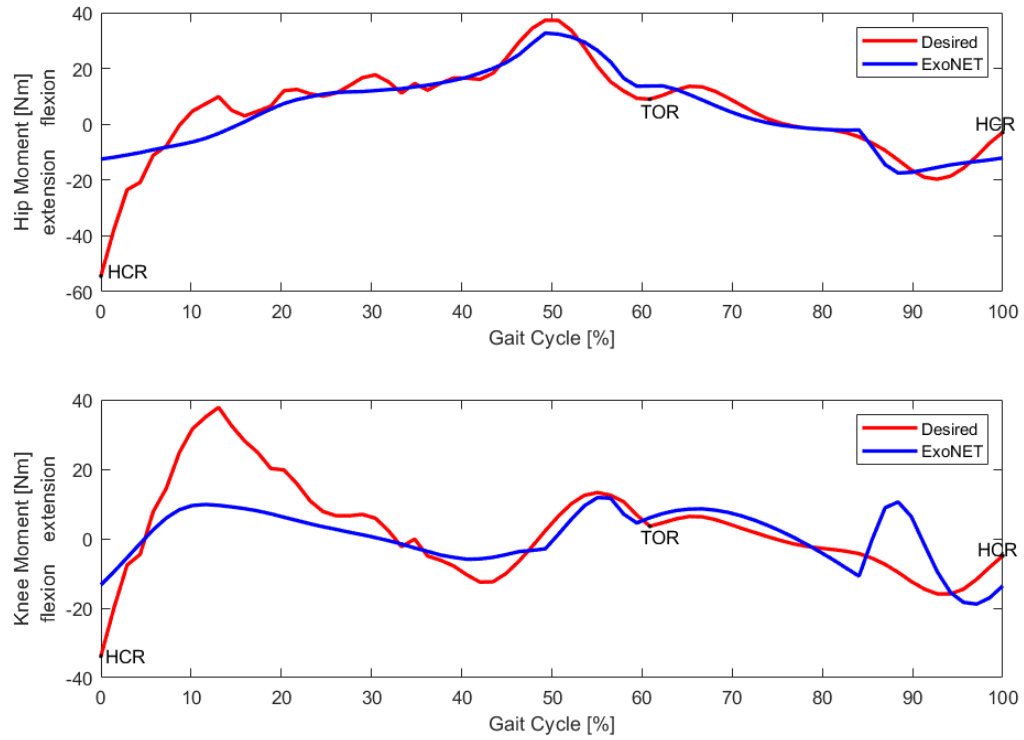


Figure 16: Torque field produced by the right leg of a healthy person during walking (in red) and simulated torque field generated by the two-element ExoNET system (in blue) with respect to the percentage of gait cycle. The points of TOR (Toe Off Right) and of HCR (Heel Contact Right) are highlighted.

5.1.3 Three-element ExoNET System

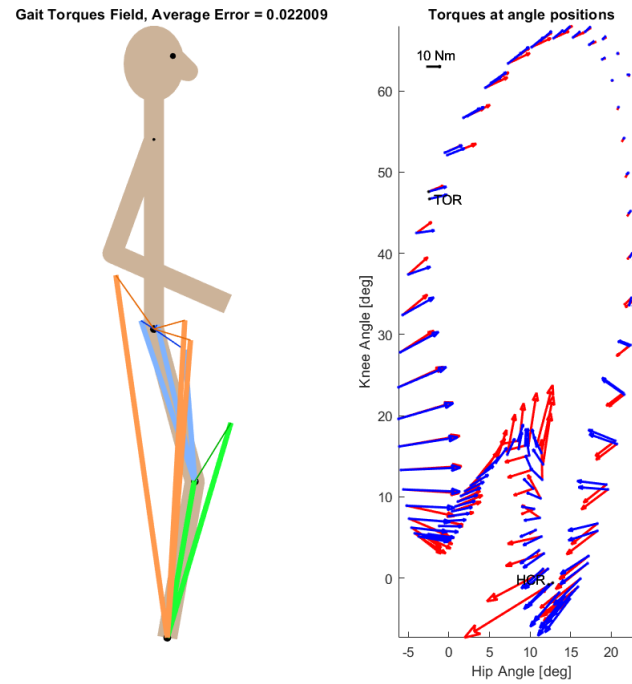


Figure 17: Arrangement of the three-element ExoNET system and associated torques generated by the device. To the left, a schematic of the body and the arrangement of the ExoNET, to the right, the torques created by the device (in blue) and the desired torques (in red). The joints (shoulder, hip, knee and ankle) are represented as black dots. Each MARIONET is represented as a line of a different color (blue, green and orange).

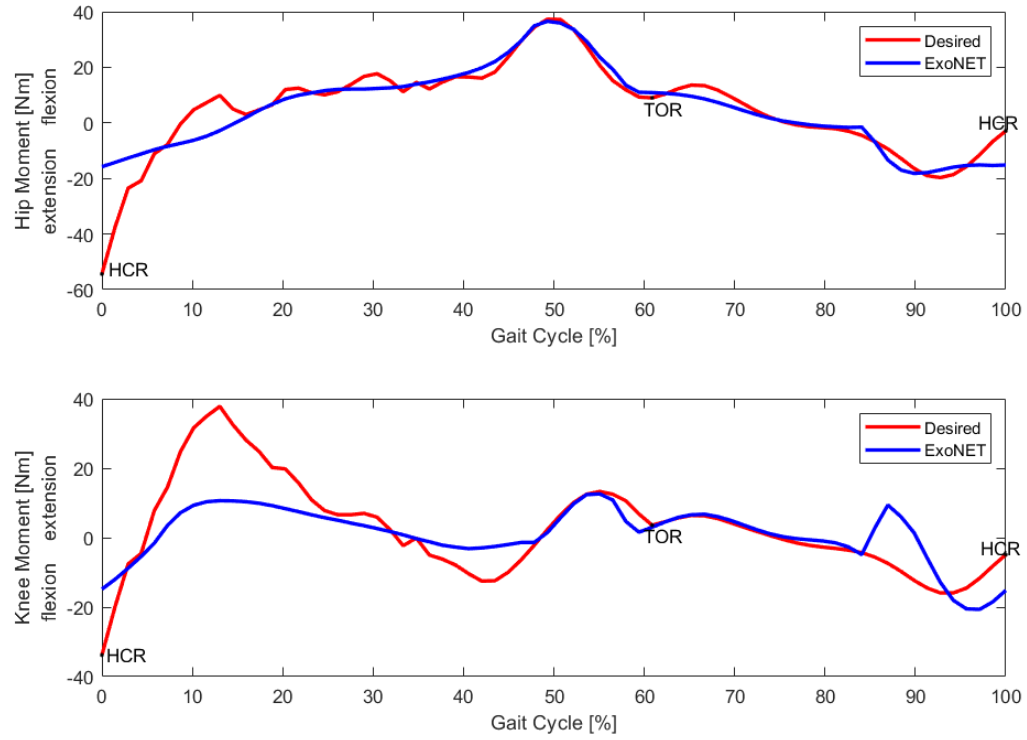


Figure 18: Torque field produced by the right leg of a healthy person during walking (in red) and simulated torque field generated by the three-element ExoNET system (in blue) with respect to the percentage of gait cycle. The points of TOR (Toe Off Right) and of HCR (Heel Contact Right) are highlighted.

It can be seen that by adding more elements, and creating a network of springs, the resulting torque field shows better fit to the desired function.

5.1.4 Error Distribution

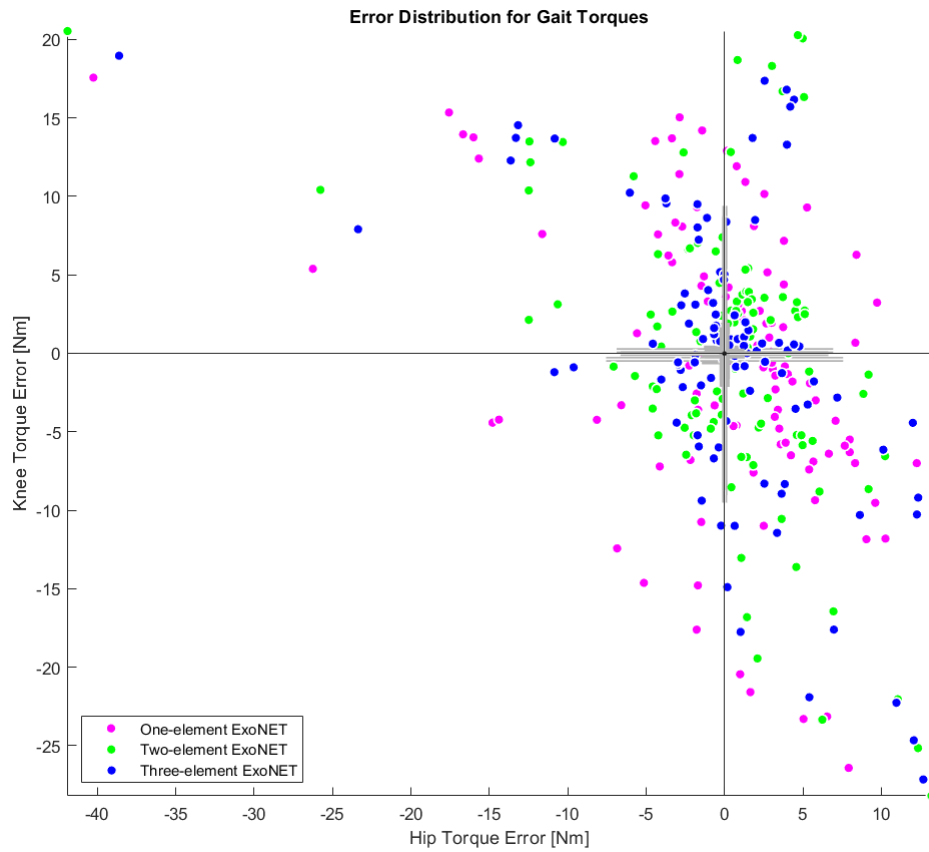


Figure 19: Knee torque error (difference between the knee desired torques and the knee actual torques) versus hip torque error (difference between the hip desired torques and the hip actual torques) for the different configurations of the ExoNET system. Each point represents an instant of the gait cycle.

To give a better understanding on how all the data points from the previous figures contribute to the average error, the error distribution for the different configurations of the ExoNET system is shown in Figure 19.

5.2 Optimization Results for Bovi et al.’s data

At first, the optimization algorithm was executed for an ExoNET system made of only one elastic element per joint, then the number of stacked MARIONETs was increased to two and three elastic elements per joint. A schematic of the human body is used to visualize how the elastic elements, in green, orange and blue, should be positioned on the lower extremity in order to provide the assistive torques to the joints. The torques created by such an arrangement of the device during the gait cycle are plotted in blue, while the desired torques are plotted in red. During the movement of the leg, the moment arm of the springs is rigid and remains in place, while the springs engage and disengage based on the joint’s position.

5.2.1 One-element ExoNET System

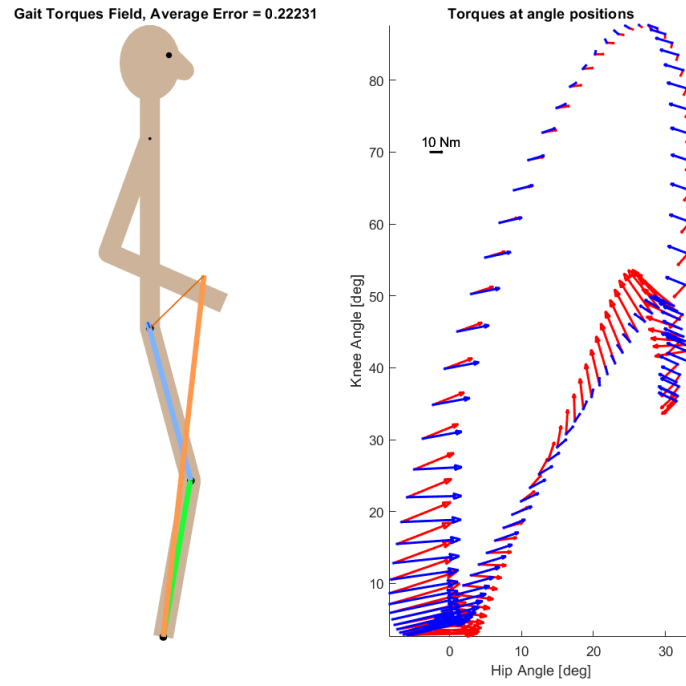


Figure 20: Arrangement of the one-element ExoNET system and associated torques generated by the device. To the left, a schematic of the body and the arrangement of the ExoNET, to the right, the torques created by the device (in blue) and the desired torques (in red). The joints (shoulder, hip, knee and ankle) are represented as black dots. Each MARIONET is represented as a line of a different color (blue, green and orange).

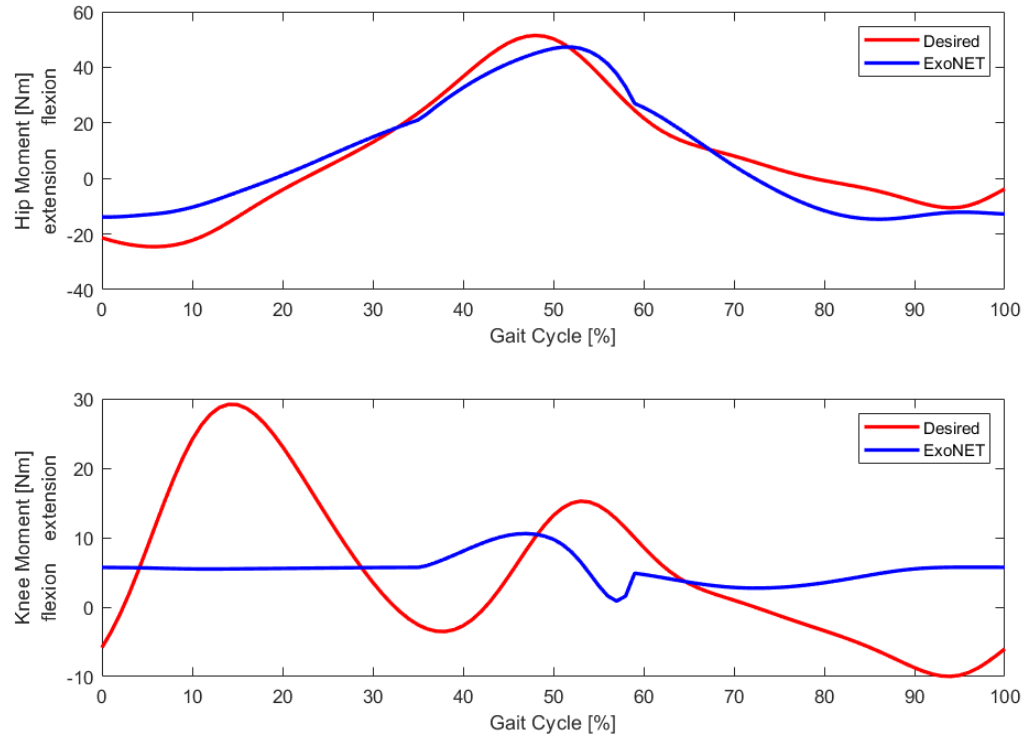


Figure 21: Torque field produced by the right leg of a healthy person during walking (in red) and simulated torque field generated by the one-element ExoNET system (in blue) with respect to the percentage of gait cycle. The points of TOR (Toe Off Right) and of HCR (Heel Contact Right) are highlighted.

5.2.2 Two-element ExoNET System

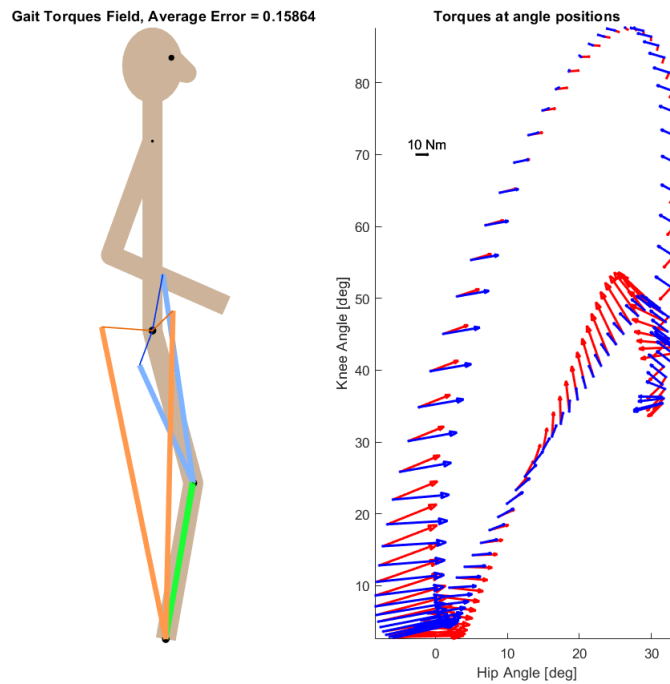


Figure 22: Arrangement of the two-element ExoNET system and associated torques generated by the device. To the left, a schematic of the body and the arrangement of the ExoNET, to the right, the torques created by the device (in blue) and the desired torques (in red). The joints (shoulder, hip, knee and ankle) are represented as black dots. Each MARIONET is represented as a line of a different color (blue, green and orange).

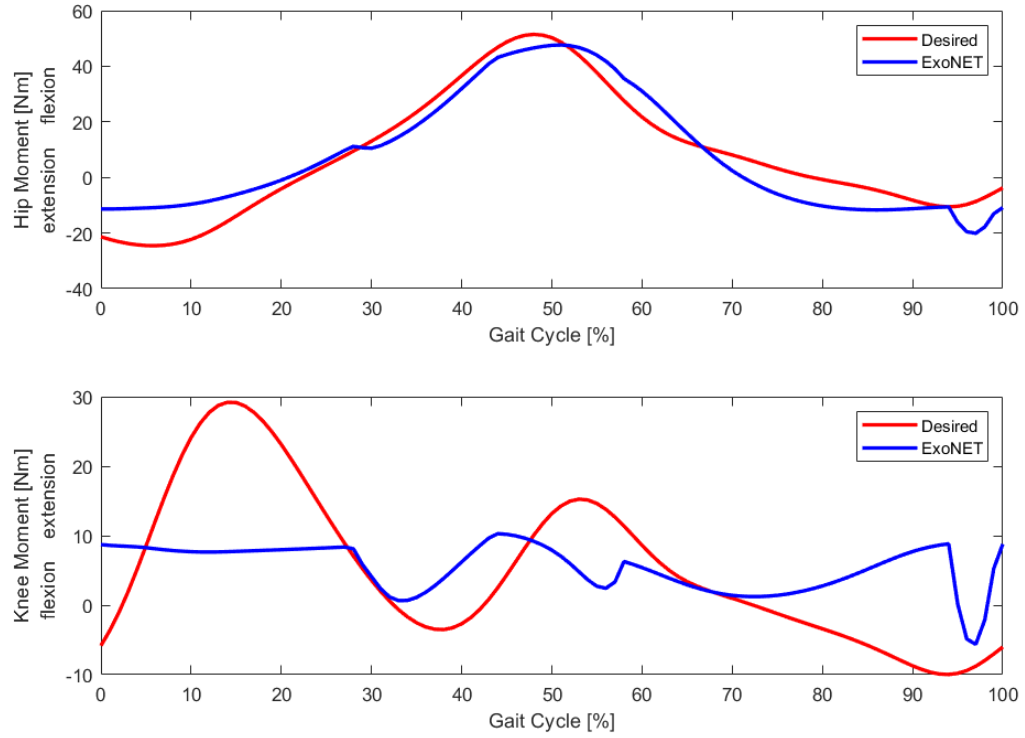


Figure 23: Torque field produced by the right leg of a healthy person during walking (in red) and simulated torque field generated by the two-element ExoNET system (in blue) with respect to the percentage of gait cycle. The points of TOR (Toe Off Right) and of HCR (Heel Contact Right) are highlighted.

5.2.3 Three-element ExoNET System

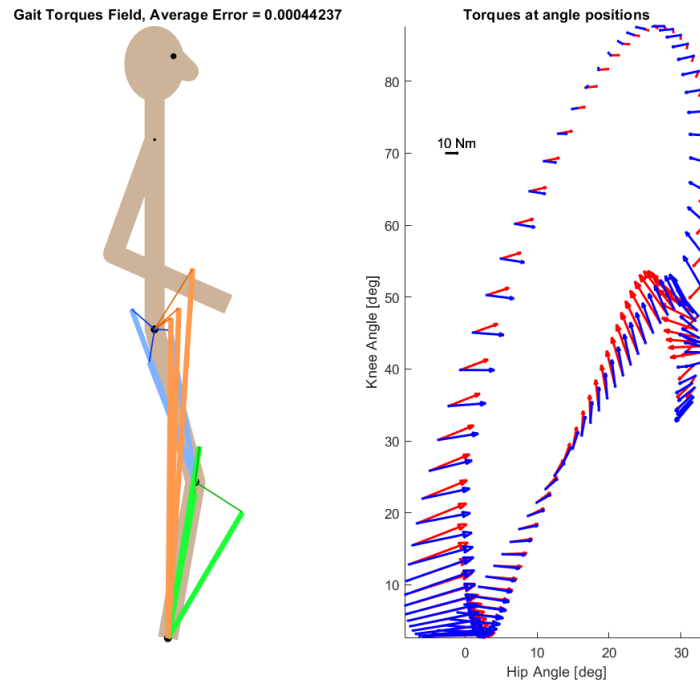


Figure 24: Arrangement of the three-element ExoNET system and associated torques generated by the device. To the left, a schematic of the body and the arrangement of the ExoNET, to the right, the torques created by the device (in blue) and the desired torques (in red). The joints (shoulder, hip, knee and ankle) are represented as black dots. Each MARIONET is represented as a line of a different color (blue, green and orange).

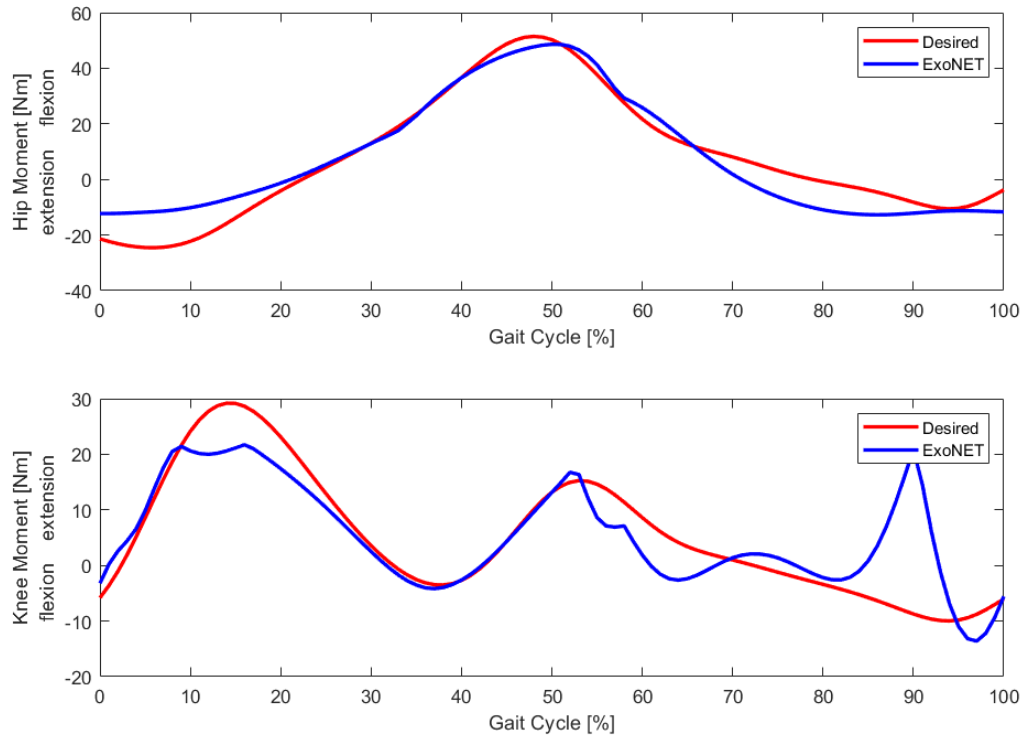


Figure 25: Torque field produced by the right leg of a healthy person during walking (in red) and simulated torque field generated by the three-element ExoNET system (in blue) with respect to the percentage of gait cycle. The points of TOR (Toe Off Right) and of HCR (Heel Contact Right) are highlighted.

It can be seen that by adding more elements, and creating a network of springs, the resulting torque field shows better fit to the desired function.

5.2.4 Error Distribution

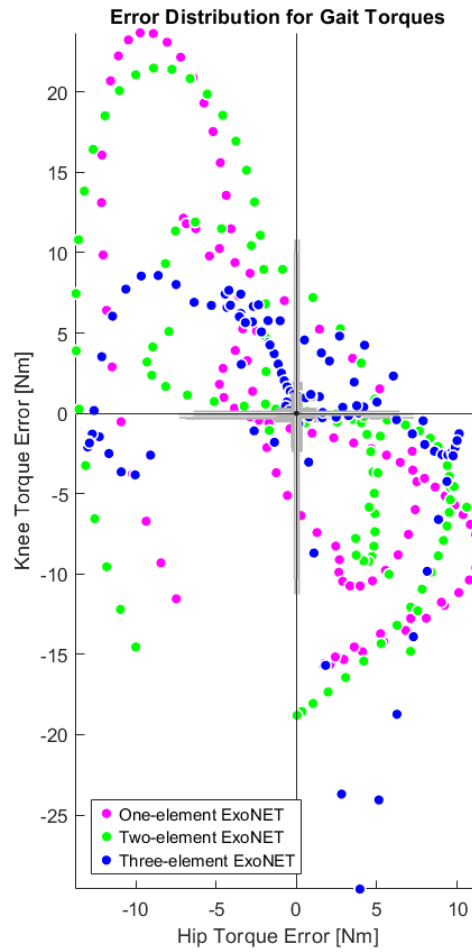


Figure 26: Knee torque error (difference between the knee desired torques and the knee actual torques) versus hip torque error (difference between the hip desired torques and the hip actual torques) for the different configurations of the ExoNET system. Each point represents an instant of the gait cycle.

To give a better understanding on how all the data points from the previous figures contribute to the average error, the error distribution for the different configurations of the ExoNET system is shown in Figure 26.

5.3 Sensitivity Analysis

A further investigation on the ExoNET system consisted of an analysis of the ExoNET's sensitivity to small changes in the torque field. The desired torques were distorted in a systematic way using a uniform noise of ± 1 Nm, in order to see how much the ExoNET system was sensitive to variations on the desired function. The goal was to see if, aside from small variations on the average error, the configuration of the ExoNET would remain nearly the same. This would mean that the optimizer is sure about the solution in output and not highly variable. Eight different perturbation combinations were created by adding and subtracting 1 Nm alternatively to the hip torque profile and to the knee torque profile. In Figure 28, the results of the sensitivity analysis are shown. In Figure 27, it's shown how the average magnitude of the error, namely the difference between the desired torques and the actual torques, varied along with all the different perturbation combinations, with respect to the non-distorted configuration (5).

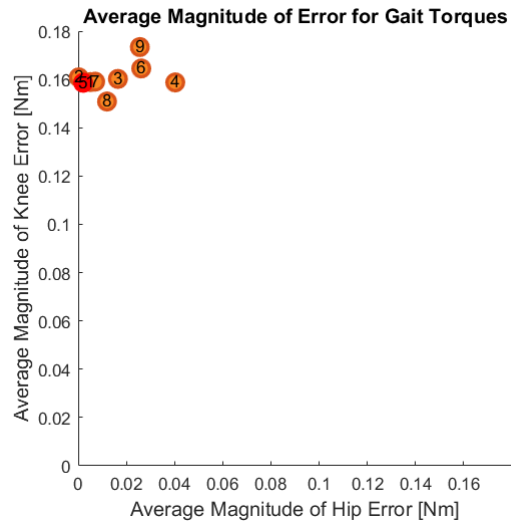


Figure 27: Average magnitude of the error, namely the difference between the desired torques and the actual torques, across all the perturbation combinations. The non-distorted configuration (5) is highlighted in red.

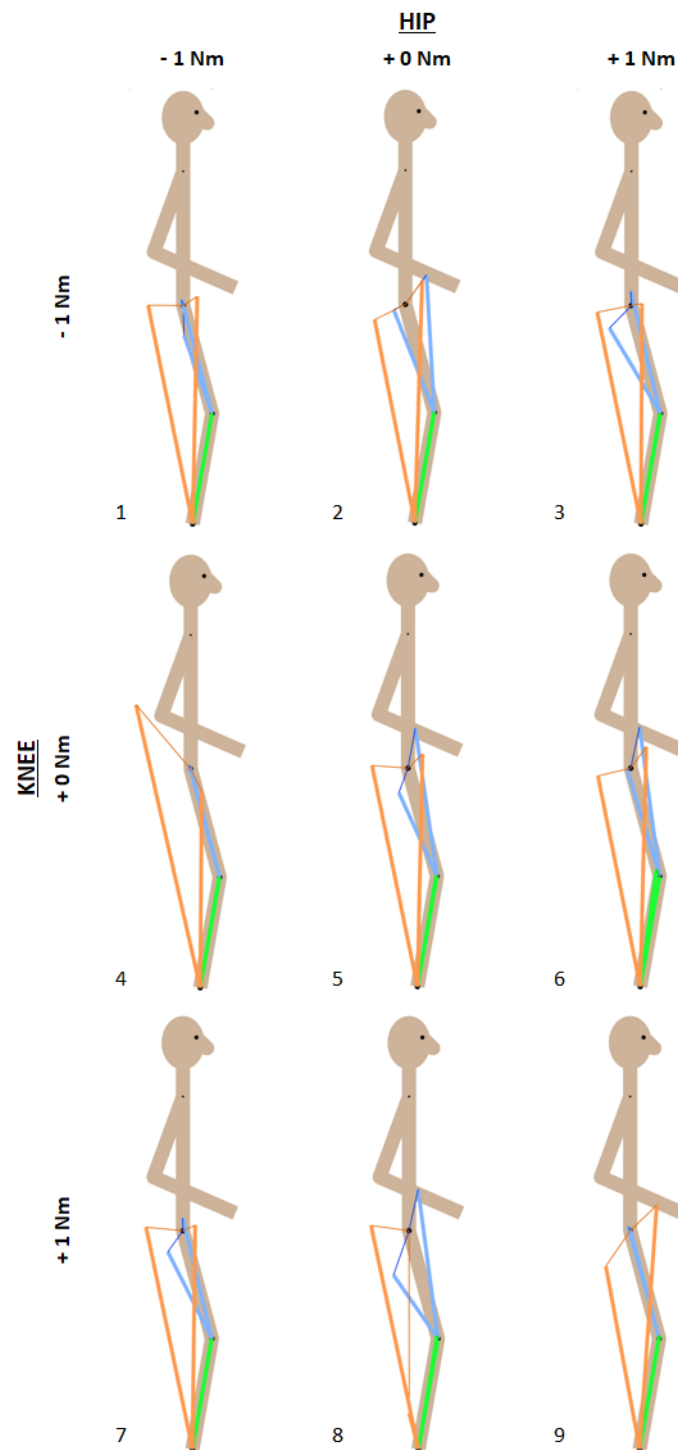


Figure 28: Arrangement of the two-element ExoNET system for different combinations of perturbation on the desired torque field.

CHAPTER 6

DISCUSSION

Parts of this chapter were previously published as Malizia, B., Ryali, P., and Patton, J. L.: Passive Exotendon Spring Elements can replace Muscle Torque during Gait. In 2020 8th IEEE RAS/EMBS International Conference for Biomedical Robotics and Biomechatronics (BioRob), pages 773-778, 2020.

6.1 Optimization Results

The residual, namely the difference between the desired torques and the actual torques, is a vector that quantitatively provides the contribution required from the muscles when wearing the device, because it indicates what cannot be stored in the springs. The figures presented in Chapter 5 show that the decrease in the average error is the same for the two datasets. If the ExoNET torque profile shows a harsh non-linearity, it could mean that one or more springs are going slack, but there is the possibility that the optimization algorithm exploits this behaviour to approximate the desired torque field. The elastic elements that end up having zero moment arm are not needed, because they don't contribute to the total torque exerted by the device, so they may not be built and, this way, the bulkiness of the device could be decreased.

6.2 Error Distribution

Figure 26 shows that the error distribution for Bovi et al.'s dataset for a three-element ExoNET system is more evenly distributed around zero, while the distribution is similar for

the one- and the two-element ExoNET system. For the hip joint, since hip flexion is considered positive and hip extension is considered negative, a positive error means that the system is hip extension deficient, while a negative error means that the system is hip flexion deficient. For the knee joint, since knee extension is considered positive and knee flexion is considered negative, a positive error means that the system is knee flexion deficient, while a negative error means that the system is knee extension deficient. Thus, Figure 26 points out that having a knee extension deficiency (negative error) is more likely. In Figure 19, it looks like that the error distribution doesn't change much for the three-element ExoNET system. The difference in the solution could be due to the difference in the dataset, that is less smooth compared to the one provided by Bovi et al., which is closer to the look of gait data acquired in a modern laboratory.

6.3 Sensitivity Analysis

It appears from Figure 28 that the geometry of the ExoNET system does not change much if the desired torque field is changed by just a little bit. Figure 27 shows that the average magnitude of the hip error is slightly lower compared to the average magnitude of the knee error, but still close to zero. This could be due to the fact that the hip torque profile is a unimodal pattern, so it could be easier to approximate.

6.4 Conclusion

The ExoNET is a multidimensional spring system. By using multidimensional springs that store and return energy during the gait cycle, the active energy input from the muscles can decrease. This way, the use of the muscles can be reduced and thus the metabolic cost of

walking could be reduced. The results presented in this work show that it is possible to create a passive torque field from elastic elements that approximates the muscular torque demand for the walking cycle. The simulated torque profiles generated by the ExoNET system suggest its potential for delivering assistive torques during gait rehabilitation. The fact that these torque fields showed limitations during the stance phase could be a disadvantage for some patient groups who need specific assistance during this phase, however, other deficits could be addressed, like the ones occurring during the swing phase, such as Stiff-Knee Gait (SKG). Moreover, assistance during the swing phase is more needed by stroke patients. This research aims at building a user-friendly, customizable, safe and inexpensive device that overcomes the need for motors and controllers, capable of providing assistive torques to patients with motor deficits. The need for a customizable device comes from the fact that the desired torques for rehabilitation are different from patient to patient and they could also change with time as the patient recovers. The proposed ExoNET system has the potential to be a simple and inexpensive device, easily adjustable by therapists and capable of providing assistive torques to patients with motor deficits. Further investigations in a clinical setting would be needed to quantify the time required to perform the customization of the device for each patient and for each stage of the recovery.

CHAPTER 7

FUTURE WORK

Parts of this chapter were previously published as Malizia, B., Ryali, P., and Patton, J. L.: Passive Exotendon Spring Elements can replace Muscle Torque during Gait. In 2020 8th IEEE RAS/EMBS International Conference for Biomedical Robotics and Biomechatronics (BioRob), pages 773-778, 2020.

In the presented optimization algorithm, the tunable parameters were the distance between the joint's CoR and the point of attachment of the spring (R), the angle between R and the vertical line (θ) and the resting length of the spring (L_0), while the spring stiffness was kept constant. However, spring stiffness could be considered as another parameter to be optimized by the algorithm. Moreover, the elastic elements here considered were pulling elements (each elastic element exerts a pulling tension T on the respective joint), but another possibility would be to consider also pushing or rotational elements.

7.1 Dynamic Simulation

A future development of this work may concern the implementation of a Dynamic Simulation through Musculoskeletal Models by using the software SimWise-4D, to validate the results of the optimization obtained from the MATLAB software. A simple model with solid elements could be used, composed of pelvis, thigh, shank and foot, and springs could be applied to

reproduce what happens when wearing the ExoNET. Since the ExoNET device can be used to produce torques in addition to the ones generated by the subject, it could be of interest to visualize in a dynamic simulation the additional torques applied to the patient. The goal would be to simulate the effect of the ExoNET on the model of a human subject, in order to test, validate and also design the system.

7.2 Preliminary Prototype of the ExoNET

Another future development could be the realization of a functional prototype of the ExoNET system. In Figure 29 and Figure 30, a preliminary non-functional prototype of the ExoNET is shown.

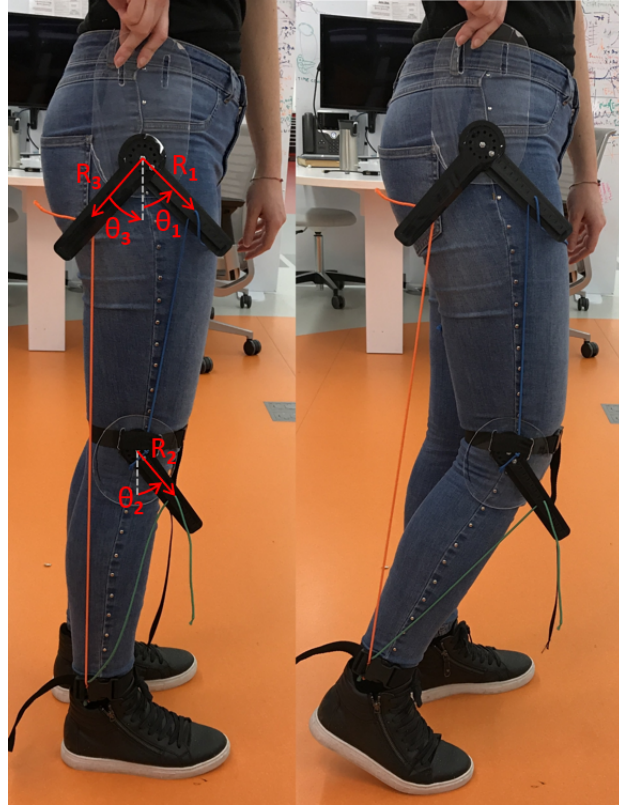


Figure 29: Physical non-functional prototype of the ExoNET made by one elastic element per joint. The parameters that can be adjusted on the ExoNET are indicated in red. ©2020 IEEE.

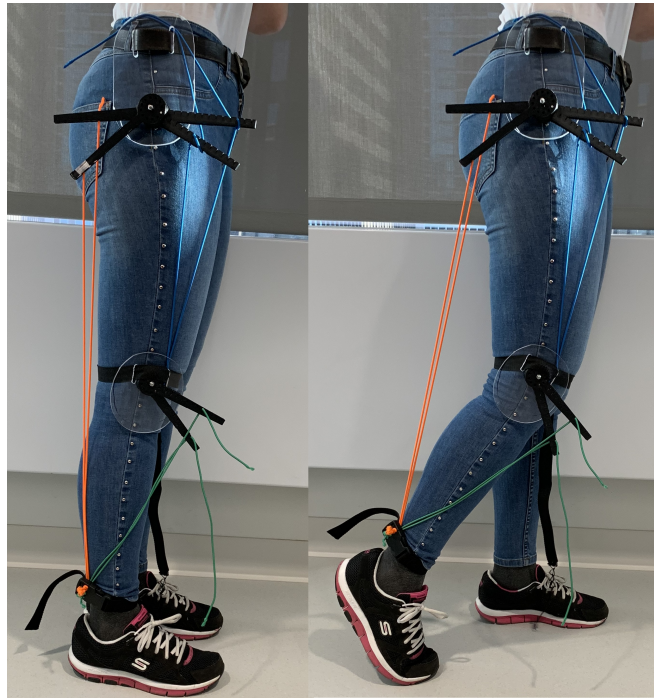


Figure 30: Physical non-functional prototype of the ExoNET made by two elastic elements per joint.

This prototype was built with very inexpensive materials, such as plexiglass and commercially available elastic cords (bungee cords), and it could be mounted on a belt thanks to the presence of two slots at the waist level. The need to adjust the moment arms of the elastic elements was addressed by using 3D printed rotators, into which the bungee cords were inserted. Plexiglass plates were cut and shaped to form the rigid boards to which the black rotators were attached. The two plexiglass boards were assembled so that the CoRs of the rotators were approximately superimposed on the CoRs of the hip and knee joints. The black rotators

were fixated to the plexiglass boards with screws and presented a series of equally spaced holes through which the bungee cords could be inserted. These rotators allow the tuning of the parameters R and θ , indeed, the distance between the CoR of the joint and the point where the spring is inserted (R) can be adjusted by inserting the bungee cord in different holes of the rotator and the angle between R and the vertical (θ) can be adjusted by rotating the rotators by 360 degrees. Therefore, the optimal parameters (R , θ , L_0) returned by the optimization algorithm for each elastic element of the ExoNET can be used to arrange each rotator and each bungee cord accordingly. By stacking more rotators on the same plexiglass board, it's possible to create ExoNET systems made of multiple elastic elements per joint. For the realization of this prototype, bungee cords were used, but elastic elements with higher stiffness could also be used, e.g. metal springs, which would also have a behavior more similar to ideal springs. The presented prototype was not a functional prototype and is shown just as a proof of concept to demonstrate that the ExoNET system can be implemented in a wearable device.



Next steps to further investigate the potentiality of this ExoNET system could include the realization of a functional prototype to be tested on a treadmill, in order to answer preliminary questions, such as: is the device comfortable to wear? Does it affect gait? Do we have gait symmetry when wearing the device? Does it make gait easier?






©2020 IEEE. Reprinted, with permission, from Beatrice Malizia, Partha Ryali and James L. Patton, "Passive Exotendon Spring Elements can replace Muscle Torque during Gait", in 2020 8th IEEE RAS/EMBS International Conference for Biomedical Robotics and Biomechatronics (BioRob), Nov 29 - Dec 1, 2020.


APPENDIX

PERMISSION TO REUSE IEEE MATERIAL

https://s100.copyright.com/AppDispatchServlet#formTop

 Home
  Help
  Email Support
  Sign in
  Create Account



Requesting permission to reuse content from an IEEE publication

Passive Exotendon Spring Elements can replace Muscle Torque during Gait

Conference Proceedings:
2020 8th IEEE RAS/EMBS International Conference for Biomedical Robotics and Biomechatronics (BioRob)

Author: Beatrice Malizia

Publisher: IEEE

Date: Nov. 2020

Copyright © 2020, IEEE

Thesis / Dissertation Reuse

The IEEE does not require individuals working on a thesis to obtain a formal reuse license, however, you may print out this statement to be used as a permission grant:

Requirements to be followed when using any portion (e.g., figure, graph, table, or textual material) of an IEEE copyrighted paper in a thesis:

- 1) In the case of textual material (e.g., using short quotes or referring to the work within these papers) users must give full credit to the original source (author, paper, publication) followed by the IEEE copyright line © 2011 IEEE.
- 2) In the case of illustrations or tabular material, we require that the copyright line © [Year of original publication] IEEE appear prominently with each reprinted figure and/or table.
- 3) If a substantial portion of the original paper is to be used, and if you are not the senior author, also obtain the senior author's approval.

Requirements to be followed when using an entire IEEE copyrighted paper in a thesis:

- 1) The following IEEE copyright/ credit notice should be placed prominently in the references: © [year of original publication] IEEE. Reprinted, with permission, from [author names, paper title, IEEE publication title, and month/year of publication]
- 2) Only the accepted version of an IEEE copyrighted paper can be used when posting the paper or your thesis on-line.
- 3) In placing the thesis on the author's university website, please display the following message in a prominent place on the website: In reference to IEEE copyrighted material which is used with permission in this thesis, the IEEE does not endorse any of [university/educational entity's name goes here]'s products or services. Internal or personal use of this material is permitted. If interested in reprinting/republishing IEEE copyrighted material for advertising or promotional purposes or for creating new collective works for resale or redistribution, please go to http://www.ieee.org/publications_standards/publications/rights/rights_link.html to learn how to obtain a License from RightsLink.

If applicable, University Microfilms and/or ProQuest Library, or the Archives of Canada may supply single copies of the dissertation.

CITED LITERATURE

1. Malizia, B., Ryali, P., and Patton, J. L.: Passive Exotendon Spring Elements can replace Muscle Torque during Gait. In 2020 8th IEEE RAS/EMBS International Conference for Biomedical Robotics and Biomechatronics (BioRob), pages 773–778, 2020.
2. Auberger, R., Pobatschnig, B., Russold, M., Riener, R., and Dietl, H.: Activities with a Microprocessor-Controlled Leg Brace for Patients with Lower Limb Paralysis: A Series of Case Studies. IEEE Transactions on Medical Robotics and Bionics, pages 1–1, 2020.
3. Mustafaoglu, R., Erhan, B., Yeldan, I., Gunduz, B., and Tarakci, E.: Does robot-assisted gait training improve mobility, activities of daily living and quality of life in stroke? A single-blinded, randomized controlled trial. Acta Neurologica Belgica, 120(2):335–344, April 2020.
4. Tanaka, E., Iwasaki, Y., Saegusa, S., and Yuge, L.: Gait and ADL rehabilitation using a whole body motion support type mobile suit evaluated by cerebral activity. pages 3286–3291. IEEE, October 2012.
5. Riener, R., Lünenburger, L., Maier, I., Colombo, G., and Dietz, V.: Locomotor Training in Subjects with Sensori-Motor Deficits: An Overview of the Robotic Gait Orthosis Lokomat. Journal of Healthcare Engineering, 1:197–216, June 2010.
6. Bach Baunsgaard, C., Vig Nissen, U., Katrin Brust, A., Frotzler, A., Ribeill, C., Kalke, Y.-B., León, N., Gómez, B., Samuelsson, K., Antepohl, W., Holmström, U., Marklund, N., Glott, T., Opheim, A., Benito, J., Murillo, N., Nachtegaal, J., Faber, W., and Biering-Sørensen, F.: Gait training after spinal cord injury: safety, feasibility and gait function following 8 weeks of training with the exoskeletons from Ekso Bionics. Spinal Cord, 56(2):106–116, February 2018.
7. Awad, L., Esquenazi, A., Francisco, G., Nolan, K., and Jayaraman, A.: The ReWalk ReStoreTM soft robotic exosuit: a multi-site clinical trial of the safety, reliability, and feasibility of exosuit-augmented post-stroke gait rehabilitation. Journal of NeuroEngineering and Rehabilitation, 17, December 2020.

CITED LITERATURE (continued)

8. Simpson, C. S., Welker, C. G., Uhlich, S. D., Sketch, S. M., Jackson, R. W., Delp, S. L., Collins, S. H., Selinger, J. C., and Hawkes, E. W.: Connecting the legs with a spring improves human running economy. Journal of Experimental Biology, 222(17), 2019.
9. Agrawal, S., Banala, S., and Fattah, A.: A Gravity Balancing Passive Exoskeleton for the Human Leg. August 2006.
10. Collins, S. H., Wiggin, M. B., and Sawicki, G.: Reducing the energy cost of human walking using an unpowered exoskeleton. Nature, 522:212–215, 2015.
11. Barazesh, H. and Ahmad Sharbafi, M.: A biarticular passive exosuit to support balance control can reduce metabolic cost of walking. Bioinspiration and Biomimetics, 15, January 2020.
12. Sulzer, J. S., Roiz, R. A., Peshkin, M. A., and Patton, J. L.: A Highly Backdrivable, Lightweight Knee Actuator for Investigating Gait in Stroke. IEEE Transactions on Robotics, 25(3):539–548, 2009.
13. Farley, C. T., Glasheen, J., and McMahon, T. A.: Running springs: speed and animal size. Journal of Experimental Biology, 185(1):71–86, 1993.
14. McMahon, T. A.: Spring-Like Properties of Muscles and Reflexes in Running. In Multiple Muscle Systems, eds. J. M. Winters and S. L.-Y. Woo, pages 578–590. Springer-Verlag, 1990.
15. Kerdok, A. E., Biewener, A. A., McMahon, T. A., Weyand, P. G., and Herr, H. M.: Energetics and mechanics of human running on surfaces of different stiffnesses. Journal of Applied Physiology, 92(2):469–478, 2002.
16. Sulzer, J. S., Peshkin, M. A., and Patton, J. L.: MARIONET: An Exotendon-Driven Rotary Series Elastic Actuator for Exerting Joint Torque. IEEE 9th International Conference on Rehabilitation Robotics, pages 103–108, January 2005.
17. Van Ingen Schenau, G. J., Bobbert, M. F., and Van Soest, A. J.: The Unique Action of Bi-Articular Muscles in Leg Extensions. In Multiple Muscle Systems, eds. J. M. Winters and S. L.-Y. Woo, page 639–652. Springer-Verlag, 1990.
18. Gielen, S., Van Ingen Schenau, G. J., Tax, T., and Theeuwes, M.: The Activation of Mono- and Bi-Articular Muscles in Multi-Joint Movements. In Multiple Muscle Systems, eds. J. M. Winters and S. L.-Y. Woo, pages 302–311. Springer-Verlag, 1990.

CITED LITERATURE (continued)

19. Ryali, P., Carella, T., McDermed, D., Perizes, V., and Patton, J. L.: A Theoretical Framework for a Network of Elastic Elements Generating Arbitrary Torque Fields. In 2020 8th IEEE RAS/EMBS International Conference for Biomedical Robotics and Biomechatronics (BioRob), pages 286–291. IEEE, 2020.
20. Winter, D. A.: Biomechanics and Motor Control of Human Movement. Wiley, 4th edition, 2009.
21. Bovi, G., Rabuffetti, M., Mazzoleni, P., and Ferrarin, M.: A multiple-task gait analysis approach: Kinematic, kinetic and EMG reference data for healthy young and adult subjects. Gait and Posture, 33(1):6–13, January 2011.
22. Abbas, A.: 19 - Fuzzy logic control in support of autonomous navigation of humanitarian de-mining robots. In Using Robots in Hazardous Environments, eds. Y. Baudoin and M. K. Habib, pages 453–475. Woodhead Publishing, 2011.
23. Martínez, C. M. and Cao, D.: 2 - Integrated energy management for electrified vehicles. In Ihorizon-Enabled Energy Management for Electrified Vehicles, eds. C. M. Martínez and D. Cao, pages 15–75. Butterworth-Heinemann, 2019.
24. Lee, I. and Yang, J.: 2.27 - Common Clustering Algorithms. In Comprehensive Chemometrics, eds. S. D. Brown, R. Tauler, and B. Walczak, pages 577–618. Oxford, Elsevier, 2009.
25. Murray-Smith, D. J.: 6 - Experimental modelling: system identification, parameter estimation and model optimisation techniques. In Modelling and Simulation of Integrated Systems in Engineering, ed. D. J. Murray-Smith, pages 165–214. Woodhead Publishing, 2012.

VITA

NAME	Beatrice Malizia												
EDUCATION	<p>Master of Science in Bioengineering, University of Illinois at Chicago, Chicago, Illinois, 2021.</p> <p>Master of Science in Biomedical Engineering, Politecnico di Milano, Milan, Italy, 2021.</p> <p>Bachelor of Science in Biomedical Engineering, Politecnico di Milano, Milan, Italy, 2018.</p>												
LANGUAGE SKILLS	<table><tr><td>Italian</td><td>Native Speaker</td></tr><tr><td>English</td><td>Full working proficiency</td></tr><tr><td>2019/20</td><td>One year of study abroad in Chicago, Illinois</td></tr><tr><td>2018/20</td><td>Lessons and exams attended in English</td></tr><tr><td>French</td><td>Limited working proficiency</td></tr><tr><td>2018/19</td><td>Six months of study abroad in Grenoble, France</td></tr></table>	Italian	Native Speaker	English	Full working proficiency	2019/20	One year of study abroad in Chicago, Illinois	2018/20	Lessons and exams attended in English	French	Limited working proficiency	2018/19	Six months of study abroad in Grenoble, France
Italian	Native Speaker												
English	Full working proficiency												
2019/20	One year of study abroad in Chicago, Illinois												
2018/20	Lessons and exams attended in English												
French	Limited working proficiency												
2018/19	Six months of study abroad in Grenoble, France												
PUBLICATIONS	Malizia, B., Ryali, P., and Patton, J. L.: Passive Exotendon Spring Elements can replace Muscle Torque during Gait. In 2020 8th IEEE RAS/EMBS International Conference for Biomedical Robotics and Biomechatronics (BioRob), pages 773-778, 2020.												
SCHOLARSHIPS	UIC Tuition Fee Waiver sponsored by Shirley Ryan AbilityLab												